UNIVERSITEIT VAN PRETORIA
UNIVERSITY OF PRETORIA
YUNIBESITHI YA PRETORIA

HANDLING IMPROVEMENT AND ROLLOVER MITIGATION BY INFLUENCING LOAD TRANSFER

MIR890

by

Bongani Zulu

15346499

Submitted in partial fulfillment of the requirements for the degree

Master of Engineering (Mechanical Engineering)

in the

Department of Mechanical and Aeronautical Engineering

Faculty of Engineering, Built Environment and Information Technology

UNIVERSITY OF PRETORIA

ABSTRACT

HANDLING IMPROVEMENT AND ROLLOVER MITIGATION BY INFLUENCING LOAD TRANSFER

by

Bongani Zulu

Supervisor:	Prof. Schalk Els
Co-Supervisor:	Dr Herman Hamersma
Department:	Mechanical and Aeronautical Engineering
University:	University of Pretoria
Degree:	Master of Engineering (Mechanical Engineering)
Keywords	Lateral load transfer, understeer characteristic, ride height, suspension characteristics, full nonlinear vehicle model

The increasing popularity of SUVs in the global market has led to a corresponding increase in accidents and fatalities associated with these vehicles, particularly rollovers. Such incidents have raised concerns about the safety of SUVs and highlighted the need to develop effective strategies to mitigate their rollover propensity and handling limitations.

As such, this dissertation investigates various techniques to enhance SUV safety, with a particular focus on reducing their rollover propensity and improving their handling characteristics. To achieve this goal, a comprehensive literature review was conducted to identify the most effective strategies to improve SUV safety. Based on the findings, a control system was developed and modelled in simulation to alter the suspension characteristics and the ride height of the vehicle to improve its handling and reduce the risk of rollover.

The constant radius test was used to evaluate the control system's performance and determine the influence of changes in suspension characteristics and ride height on the vehicle's handling behaviour. The test revealed that changes in suspension characteristics and ride height significantly impact the vehicle's handling behaviour and lateral load transfer, leading to improved manoeuvrability and stability. The reduction in ride height was identified as an effective means of reducing the rollover propensity and improving the handling characteristics of SUVs, with promising results that warrant further investigation and implementation in real-world vehicles. Furthermore, the vehicle's lateral

dynamics were tested using the double lane change, where an improvement is shown with a change in the suspension settings and after using anti-roll control. The vehicle was also tested for rollover using the Fishhook 1B test, where the characteristic speed of the vehicle was obtained by investigating the suspension configurations that allowed the vehicle to pass the test.

Overall, this research makes an important contribution to developing effective strategies for enhancing SUV safety by influencing vehicle load transfer, which is crucial for reducing the number of fatalities on the road.

ACKNOWLEDGEMENTS

I would like to take this opportunity to express my heartfelt gratitude to all those who have supported and guided me throughout this journey. Your unwavering encouragement and invaluable insights have been instrumental in bringing this dissertation to fruition.

- My parents Refiloe and Dumisani Zulu for giving me the opportunity to become a university student and for the tools to persevere through the tough times.
- Professor Els for imparting the pebbles of knowledge that many dream of having. Thank you for the guidance to become a better person, academically and in all aspects of life.
- The whole of the Vehicle Dynamics Group for setting the standard for collaborative and innovative environments high. Thank you for the countless opportunities to learn and be part of the team.

Table of Contents

Nomenclature

Greek

α	Slip angle [deg]
$\ddot{\psi}$	Yaw angular acceleration [deg/s^2]
$\ddot{\varphi}$	Roll angular acceleration [deg/s^2]
δ	Steering angle [deg]
$\dot{\psi}$	Yaw rate [deg/s]
$\dot{\varphi}$	Roll rate [deg/s]
ψ	Yaw angle [deg]
ε	Roll steering coefficient
φ	Roll angle [deg]

Symbols

a	Acceleration [m/s^2]
a, b, c, e, h, l	Distance [m]
C	Cornering stiffness [N/rad]
d	Damping factor
F	Force [N]
g	Gravitational acceleration [N/rad]
h_r	Roll centre height [m]
I	Moment of inertia [kgm^2]

L Wheelbase [m]

m Mass [kg]

R Turning radius [m]

T Torque [Nm]

t Track width [m]

V Forward velocity [m/s]

Subscripts

f Front

i Inside

o Outside

r Rear

s Sprung mass

us Unsprung mass

x Longitudinal Plane

y Lateral Plane

z Vertical Plane

List of Abbreviations

AARB	Active Anti-Roll Bar
ADAMS	Automatic Dynamic Analysis of Mechanical Systems
BWR	Benedict Webb Rubin
CG	Centre of Gravity
CRT	Constant Radius Test
DLC	Double Lane Change
DOF	Degrees of Freedom
EE	Energy Equation
ESC	Electronic Stability Control
FL	Front Left
FR	Front Right
IG	Ideal Gas
ISO	International Organisation for Standardisation
LTR	Load Transfer Ratio
MATLAB	Matrix Laboratory
NHSTA	National Highway Traffic Safety Administration
RL	Rear Left
RMS	Root-Mean-Square
RR	Rear Right
SAE	Society of Automotive Engineers
SSF	Static Stability Factor
SUV	Sport Utility Vehicle
VDG	Vehicle Dynamics Group
ZMP	Zero Moment Point
$4S_4$	Four-State Semi-Active Suspension System
$4S_4$CVD	Four-State Semi-Active Suspension System with Continuously Variable Damping

List of Figures

List of Tables

1. Introduction

1.1 Background

In recent years, the global demand for sport utility vehicles (SUVs) has experienced a significant rise. These vehicles have gained popularity among consumers due to their spaciousness, comfort, and robustness. In nine years, the volume of SUVs in operation worldwide increased by close to six times the 2010 volume, reaching 200 million units in 2019. SUVs represented some 29.6 million global car sales a year later, in 2020, with electric SUVs adding another 1.1 million units sold. [Statista (2023)]

However, SUVs are also associated with an increased risk of accidents, particularly rollovers, which are considered highly dangerous. In the USA in 2021, single-vehicle rollover crashes accounted for 16 percent of occupant deaths in cars, 30 percent of occupant deaths in pickups, and 27 percent of occupant deaths in SUVs. [Insurance Institute for Highway Safety (2020)] The Insurance Institute for Highway Safety (2020) cited that in the US, 6 358 passenger vehicle occupants died in rollover crashes in 2019. Even though the bulk of the rollovers were associated with pre-rollover impact (74%), a significant fraction (26%) rolled over without having impacted anything beforehand.

The higher centre of gravity and larger size of SUVs make them more prone to poor handling and, consequently, a higher likelihood of rollovers compared to other vehicle types, which has led to a growing concern over the rising number of fatalities and injuries resulting from SUV rollovers, prompting policymakers, regulators, and safety advocates to address this issue. New safety standards and guidelines for SUVs have been developed as a response. For instance, the Australasian New Car Assessment Programme has announced that only vehicles with ESC will be given five stars from 2008 onward. In the US, legislation was passed in 2007 making ESC mandatory standard equipment for all passenger cars, multipurpose vehicles, trucks and buses with gross vehicle rating of 4,536 kg or less from model year 2012. [European Road Safety Observatory (2023)]

Despite these efforts, SUVs are associated with a higher risk of rollovers and other types of accidents. To address this issue, researchers are exploring new approaches to improve the handling and stability of SUVs, including advanced control systems, such as active suspension systems, and innovative testing methods, such as simulators and real-world testing. By enhancing the safety of SUVs, these efforts aim to reduce the number of fatalities and injuries associated with SUV accidents and improve the overall safety of the roads. These efforts are essential as the number of deaths where the vehicle is an SUV has steadily increased, as shown in Figure 1.1.

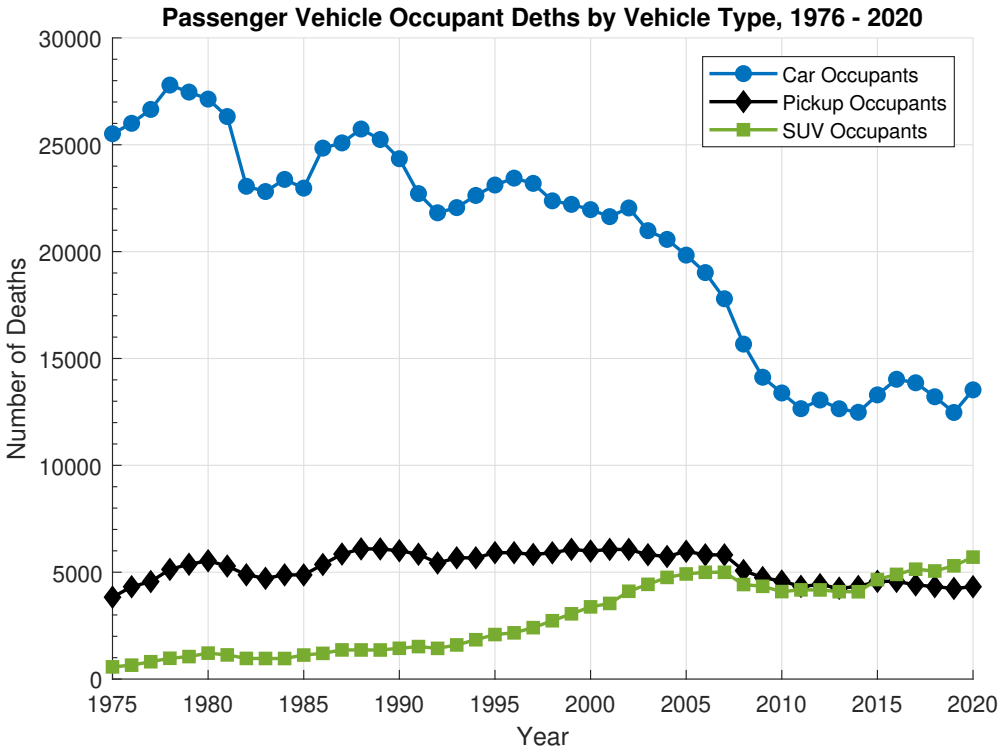

Figure 1.1. Passenger Vehicle Occupant Deaths by Vehicle Type in the USA, 1976-2020 [*Insurance Institute for Highway Safety (2020)*]

1.2 Problem Statement

Off-road vehicles are infamous for having poor handling when cornering and are prone to rollover due to a higher CG. During cornering manoeuvres, lateral forces act in the ground plane to counterbalance the lateral acceleration acting at the CG of the vehicle. The difference in the position at which these forces act creates a moment on the vehicle, which attempts to roll it towards the outside of the turn. Changing and influencing roll moments at the front and rear axle can improve handling performance against understeer and oversteer. This can be achieved by using different methods of influencing

the load transfer of the vehicle. This study will be focused on the research and understanding of the handling dynamics of an SUV. This research study's problem statement can be defined as the following objectives. Firstly, the objective is to implement vehicle rollover control methods in an ADAMS model of the Land Rover model that the Vehicle Dynamics Group developed at the University of Pretoria to improve the body roll of the vehicle and improve the handling characteristics. The research study will endeavour to answer the following research questions:

- *Can influencing the lateral load transfer of a vehicle improve the handling characteristics and decrease the rollover propensity?*
- *Can this be achieved by implementing roll control using a semi-active suspension?*
- *How will this implementation influence the steering and handling characteristics of the vehicle?*

1.3 Overview of Report

Chapter 2 includes the literature review section of this report and provides a comprehensive overview of the current state of the art related to rollover detection and prevention, handling validation and testing manoeuvres. Different approaches to limit rollover and improve handling in vehicles are also investigated. It includes a critical analysis of relevant studies, highlighting the strengths and limitations of the research and identifying any gaps in knowledge in this field.

In Chapter 3, the ADAMS simulation model is described in detail. This section provides a comprehensive overview of the model, including the different components and parameters incorporated into it, the assumptions made, and the rationale behind the modelling decisions. Additionally, this chapter provides a detailed description of the constant radius test that will be used to evaluate the rollover propensity and handling of the vehicle model. The simulation model, data acquisition process, and test conditions will be discussed in detail to provide a complete understanding of the simulation procedure.

Chapter 3 presents the results of the ADAMS simulation and data analysis. This section provides an in-depth discussion of the findings, including a detailed analysis of the simulation outputs, graphical representations of the data, and a comparison of the results with the relevant literature.

Finally, Chapter 4 provides a conclusion and recommendations for future research. This section summarises the study's findings, discusses the implications of the results, and identifies potential avenues for further research. Furthermore, it provides recommendations for applying the study findings in practice, highlighting potential limitations or improvement areas. This chapter also concludes with a discussion of the plan for future work regarding this research topic, outlining the potential directions for future research and the implications of this study for further research.

2. Literature Study

In this chapter, a comprehensive summary of the pertinent literature regarding rollover and handling is provided, encompassing various aspects such as methods for measuring rollover and handling, strategies for reducing rollover propensity and improving handling performance, characteristics associated with different suspension systems, and an introduction to the simulation model employed in this research.

2.1 Tyre Mechanics

Comprehending the interplay between tyres, their operational environment, and the resultant forces and moments at the contact patch is a crucial element in understanding the overall dynamics of a vehicle. The tyre serves three fundamental roles [Gillespie (1992)]:

- It bears the vertical load and absorbs shocks from the road.
- It generates longitudinal forces for acceleration and braking.
- It produces lateral forces for cornering.

2.1.1 Cornering Properties of Tyres

In cornering conditions, the tyre will generate a lateral force, which will also make the tyre experience lateral slip, forming a **slip angle**. The slip angle can be expressed as the angle between its direction of heading and its direction of travel during a corner. The lateral force generated in a tyre is related to the amount of slip angle experienced by the tyre. [Wong (2013)] Figure 2.1 depicts the lateral force (F_y) generated by a tyre as a function of the slip angle (α). The dashed line represents the tyre's cornering stiffness (C_α). The solid line shows the behaviour of a rolling tyre, indicating that lateral force increases with slip angle up to a peak, after which it declines. The curve for a locked wheel illustrates the lateral force as a function of the slip angle, following the formula $\mu_s F_z \sin(\alpha)$, where μ_s is the coefficient of static friction and F_z is the normal load. The diagram on the right provides a visual representation of the slip angle and direction of travel for the tyre.

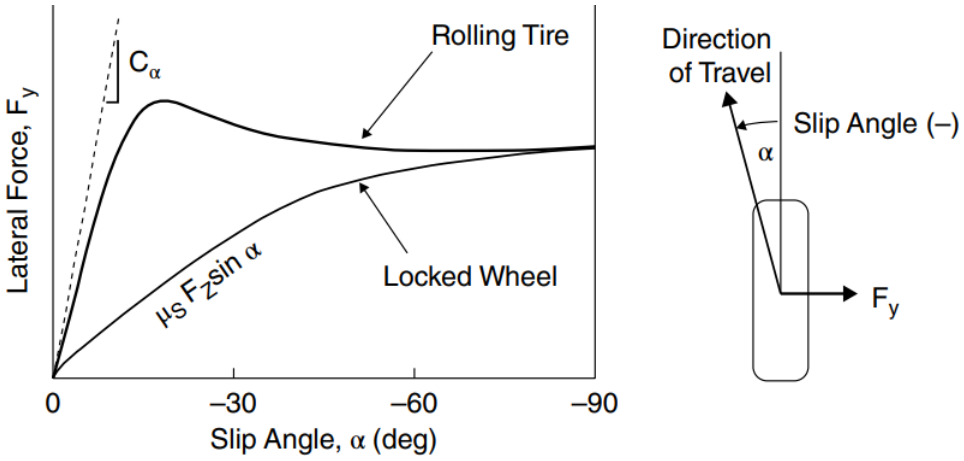

Figure 2.1. Tyre lateral force properties against slip angle for a rolling tyre and locked wheel [Gillespie (2021)]

Figure 2.2(a) illustrates that the lateral force in a tyre is a highly nonlinear function the slip angle. For small slip angles ($\alpha \leq 5$), the lateral force can be defined as:

$$F_y = C_\alpha \alpha \tag{2.1}$$

To provide a measure for comparing the cornering behaviour of different tyres, a parameter called cornering stiffness C_α is used. It is defined as the derivative of the cornering force F_y concerning slip angle α evaluated at zero slip angle [Wong (2013)]:

$$C_\alpha = \left.\frac{\partial F_y}{\partial \alpha}\right|_{\alpha=0} \tag{2.2}$$

The cornering stiffness is dependent on numerous variables such as tyre type, tyre size, width, tread, inflation pressure, vertical load and others. The normal load on the tyre strongly influences the cornering characteristics. The relationship between cornering force and normal load is evident in that, for a given slip angle, increasing the normal load generally leads to an increase in cornering force at small slip angles. However, it is important to note that this relationship is nonlinear. This is shown in Figure 2.2(a) where the slip angle can increase but the lateral force that the tyre can generate becomes almost constant. During a turning manoeuvre, the transfer of load from the inside tyre to the outside tyre will result in a reduction of the total cornering force that the axle is capable of generating. Saturation can occur with tyres where the lateral forces decrease with higher slip angles and the tyre displays nonlinear behaviour.

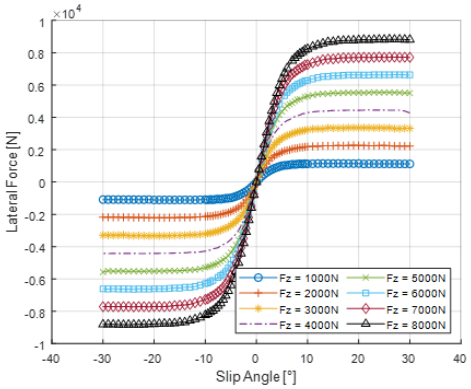

(a) Lateral Force vs Slip Angle of Pirelli Scorpion Verde Tyre [Wright et al. (2019)]

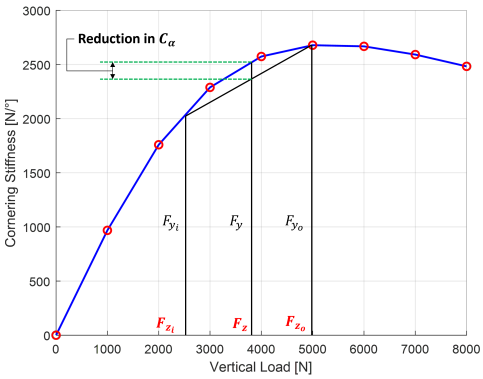

(b) Cornering Stiffness generated by Varying Vertical Load

Figure 2.2. Cornering Characteristics of Pirelli Scorpion Verde Tyre

Consider a pair of tyres on a beam axle, both experiencing a normal load F_z, as depicted in Figure 2.2(b). Each tyre generates a cornering force F_y when subjected to a specific slip angle. During a steady-state turn, the lateral load transfer causes a reduction in the normal load on the inside tyre (F_{zi}) and an increase in the normal load on the outside tyre (F_{zo}). Consequently, the combined cornering force of the two tyres becomes the average of F_{yi} and F_{yo}, which is less than F_y when the vehicle is not turning. This means that for a pair of tyres on a beam axle to generate the necessary cornering force to counteract a given centrifugal force during a turn, the lateral load transfer will require an increase in the slip angle of the tyres. Figure 2.2(b) demonstrates how the non-linearity of the tyre's cornering stiffness influences the vehicle's handling. When the vertical load on the outside tyre becomes very high, the cornering stiffness decreases, leading to a reduction in the tyre's ability to generate lateral force efficiently.

A commonly employed parameter is the cornering coefficient to assess how the normal load impacts tyre cornering performance, characterised as the cornering stiffness per unit of normal load. A typical correlation between the cornering coefficient and the normal load of the tire reveals a decrease in the cornering coefficient as the normal load increases. In addition, pneumatic tires are typically considered to exhibit load sensitivity, which implies that as the vertical load increases, the peak coefficient of friction decreases. During cornering, lateral load transfer causes the outside tyres to experience higher vertical loads and the inside tyres to experience lower loads. This load transfer impacts the available lateral grip of each tyre, influenced by their respective peak longitudinal coefficients.

As load increases on the outside tyre, its peak longitudinal coefficient may decrease, reducing its lateral force capability. Consequently, lateral load transfer reduces the overall lateral force that the tyres can produce. [Haney (2012)]. Figure 2.3 illustrates the peak longitudinal friction coefficient of a tyre and how the coefficient decreases as the vertical load on the tyre increases. This behaviour applies in steady-state conditions.

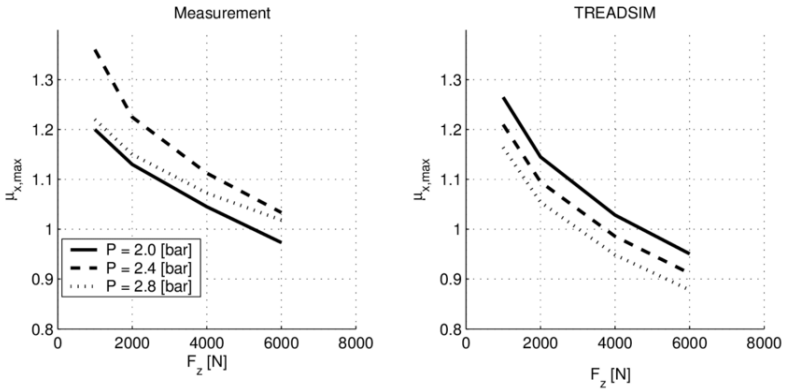

Figure 2.3. Peak longitudinal friction coefficient for a 155/70 R13 tyre [Schmeitz et al. (2005)]

In conclusion, this section underscores tyre mechanics' critical role in influencing lateral load transfer, a pivotal aspect of vehicle dynamics. The non-linear characteristics inherent in pneumatic tyres, including their response to slip angle, variations in vertical load, cornering stiffness, and friction coefficient, have been identified as central factors in understanding and predicting lateral load transfer behaviour. It becomes evident that their intricate interplay with lateral load transfer significantly shapes a vehicle's overall handling and stability.

2.2 Handling

Vehicle handling encompasses the performance characteristics and behaviour of a car in response to driver inputs, environmental conditions, and road surface variations. Effective handling is essential for safe and efficient operation, as it impacts stability, manoeuvrability, and driving dynamics. Handling focuses on the car's response to steering inputs, involving higher steer rates and larger amplitudes, covering steady-state and transient responses in the car's yaw, roll, lateral, pitch, and heave motions. [Wu et al. (2011)]

2.2.1 Steady State Cornering

2.2.1.1 Low-Speed Turning

To understand cornering, we can begin by defining low-speed turning. When vehicles turn at low speed, the tyres do not need to develop lateral forces to navigate the turn, and therefore they roll without slip angle. Due to this, the ideal turning angles for the vehicle are defined by the geometry of the turn, as shown in Figure 2.4. Assuming small angles, the average angle of the front wheels is defined as:

$$\delta = \frac{L}{R} \tag{2.3}$$

Equation 2.3 is also known as the Ackerman Angle for a given vehicle.

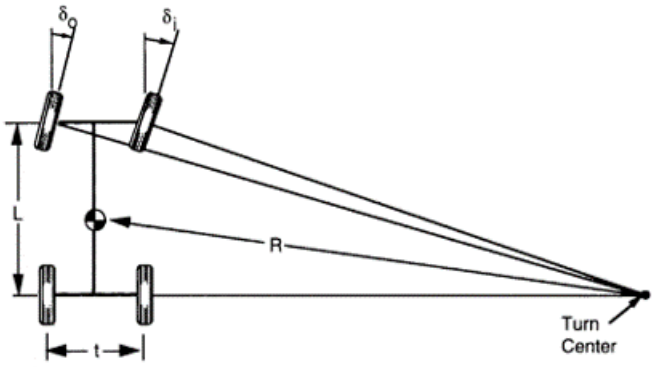

Figure 2.4. Geometry of a Turning Vehicle [*Gillespie (1992)*]

2.2.1.2 High-Speed Cornering

When cornering at high speeds, there will be a lateral acceleration that the vehicle experiences which is the centripetal acceleration acting towards the centre of the turn and the tyres must develop lateral forces to counteract this lateral acceleration therefore slip angles will be generated at each wheel. A 2-degree-of-freedom single track model can be used to depict the lateral acceleration generated, shown in Figure 2.5:

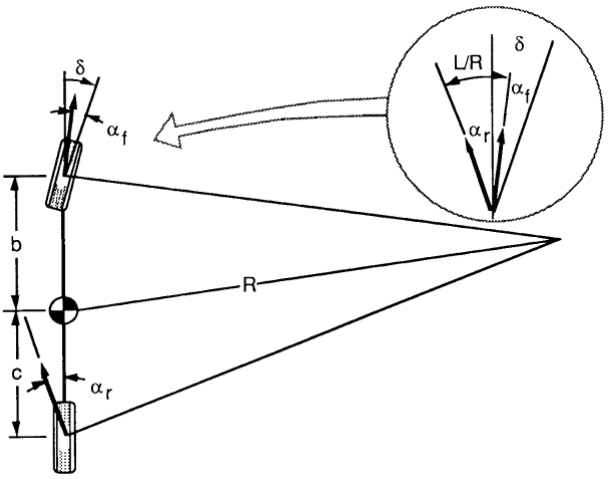

Figure 2.5. 2 Degree-of-Freedom Single Track Model Turning at High Speed [*Gillespie (1992)*]

Using the 2DOF single track model illustrated in Figure 2.5, and travelling with a forward velocity of V, the steady-state cornering equations can be derived for high-speed cornering from Newton's Second Law. The sum of the forces in the lateral direction from the tyres must be equal to the mass multiplied by the centripetal acceleration

$$\sum F_y = F_{yf} + F_{yr} = m\frac{V^2}{R} \tag{2.4}$$

Ackermann (1994) states that from analysis that the required steer angle is:

$$\delta = 57.3\frac{L}{R} + \alpha_f - \alpha_r \tag{2.5}$$

Which can be described as:

$$\delta = 57.3\frac{L}{R} + \left(\frac{W_f}{C_{\alpha_f}} - \frac{W_r}{C_{\alpha_r}}\right)\frac{V^2}{gR} \tag{2.6}$$

From Equation 2.6, the understeer gradient can be defined as:

$$K = \left(\frac{W_f}{C_{\alpha_f}} - \frac{W_r}{C_{\alpha_r}}\right) \tag{2.7}$$

The understeer gradient shows how the steering angle must be adjusted to maintain the radius of a turn based on lateral acceleration, as a function of the load on the front and rear axles.

2.2.1.3 Understeer Gradient

Equation 2.6 is often written in shorthand form as follows:

$$\delta = 57.3\frac{L}{R} + KA_y \tag{2.8}$$

The action of a vehicle navigating a turn can be divided into three main categories, namely **understeer**, **oversteer**, and **neutral steer**.

1. **Neutral steer**

   - When negotiating a constant-radius turn, a change in the steer angle of the vehicle will not be required as the speed is varied.

$$\frac{W_f}{C_{\alpha_f}} = \frac{W_r}{C_{\alpha_r}} \rightarrow K = 0 \rightarrow \alpha_f = \alpha_r \tag{2.9}$$

2. **Understeer**

   - When negotiating a constant-radius turn, the steer angle of the vehicle will have to increase as the speed is increased.

$$\frac{W_f}{C_{\alpha_f}} > \frac{W_r}{C_{\alpha_r}} \rightarrow K > 0 \rightarrow \alpha_f > \alpha_r \tag{2.10}$$

3. **Oversteer**

   - When negotiating a constant-radius turn, the steer angle of the vehicle will have to decrease as the speed is increased.

$$\frac{W_f}{C_{\alpha_f}} < \frac{W_r}{C_{\alpha_r}} \rightarrow K < 0 \rightarrow \alpha_f < \alpha_r \tag{2.11}$$

Figure 2.6 illustrates these three possibilities for steady state vehicle handling.

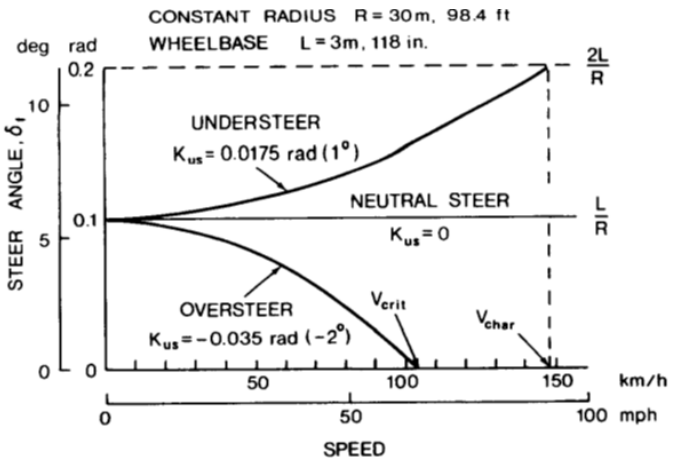

Figure 2.6. Change of Steering Angle with Speed [*Wong (2013)*]

Therefore, Equation 2.8 demonstrates the ability to determine which steering angle is required to traverse a curve with a given radius at a given lateral acceleration, which is related to the vehicle speed. Tandy et al. (2015) found that vehicle manufacturers worldwide have consensus on test protocols used to measure understeer and oversteer which also include steady state cornering with gradual changes in the steering and/or speed of the vehicle, depending on which method is used.

These include the constant radius method, the constant steering wheel angle/variable speed method, the constant speed/ variable radius method, and the constant speed/variable steer method.

2.2.2 Suspension Effects on Cornering

While tyre cornering stiffness is the foundation for understeer/oversteer equations, various vehicle design factors can impact cornering forces during lateral acceleration. Any design element influencing the cornering force at the wheel affects the vehicle's directional response directly. The suspension and steering systems play vital roles as the primary sources of these influences. This section will delve into the discussion of suspension factors that affect vehicle handling.

2.2.2.1 Lateral Load Transfer

Lateral load transfer, also referred to as lateral weight transfer, is a critical aspect of vehicle dynamics that pertains to the redistribution of vertical loads on a vehicle's tyres in response to lateral acceleration acting on the centre of gravity (CG) of the car. This phenomenon is integral to understanding the handling characteristics and stability of a vehicle during cornering manoeuvres. Essentially, lateral load transfer is the process by which the vertical load on the tyres is altered as a consequence of the forces exerted during cornering. When a vehicle negotiates a turn, the lateral acceleration induces a shift in the vertical load from the inner tyres to the outer tyres. This results in an increase in the vertical load on the tyres located on the outer side of the turn, while concurrently decreasing the vertical load on the tyres on the inner side. The magnitude of this load transfer is influenced by several factors, including the height of the vehicle's centre of gravity, the track width, the lateral acceleration, and the suspension characteristics. A higher centre of gravity or a narrower track width tends to exacerbate the extent of load transfer, potentially compromising the vehicle's grip and increasing the risk of rollover. Conversely, a lower centre of gravity and a wider track width can mitigate these effects, enhancing the vehicle's stability and handling performance. Additionally, the suspension system plays a pivotal role in modulating lateral load transfer by determining how the vehicle's body responds to the forces acting upon it during cornering.

The lateral load transfer on the car can be calculated from a free body diagram, where the vehicle is simplified to a single axle and tyres, as shown in Figure 2.6. Taking the moment equilibrium about the

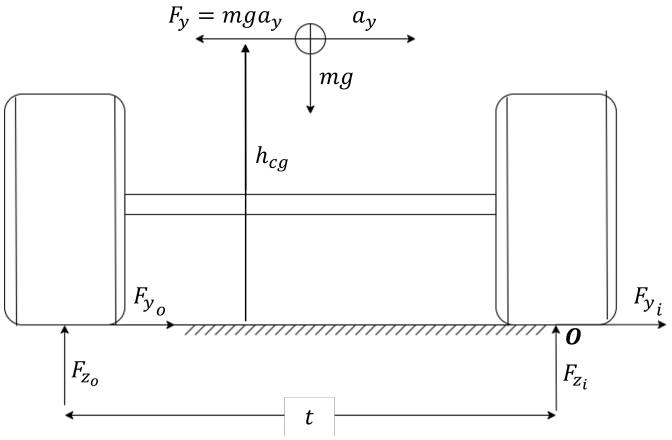

Figure 2.7. Free body diagram of a car during a right-hand turn, rear view, adapted from Milliken & Milliken (2003)

point O of the inside tyre, we can see that

$$mga_y h_{cg} - F_{z_o} t + mg\left(\frac{t}{2}\right) = 0 \rightarrow F_{z_o} t = mg\left(\frac{t}{2}\right) + mga_y h_{cg} \tag{2.12}$$

Dividing by t on both sides, we obtain:

$$F_{z_o} = \frac{mg}{2} + \frac{mga_y h_{cg}}{t} \tag{2.13}$$

Assuming a 50/50 weight distribution, $F_{z_o} = \frac{mg}{2} + \Delta F_z$. Therefore:

$$\Delta F_z = \frac{mga_y h_{cg}}{t} \tag{2.14}$$

Equation 2.14 indicates that the lateral load transfer can be influenced by the vehicle's height of the centre of gravity, the track width of the vehicle, and the mass of the vehicle. The most important factor would be h_{cg}. By affecting the height of the centre of gravity, it is possible to influence the lateral load transfer experienced by the vehicle. Lower load transfer can be achieved by lowering the CG and, conversely, an increase in load transfer can be achieved by raising the CG of the vehicle.

2.2.2.2 Roll Moment Distribution

As mentioned before, the average lateral force that both tyres generate will decrease in cornering, which leads to an increase in the slip angle of the tyres to maintain the lateral force needed to navigate the turn. If this occurs at the front tyres, then the load transfer will lead to understeer and if this occurs at the rear tyres, the load transfer will result in oversteer. The contribution to understeer or oversteer depends on the distribution of roll moments between the front and rear axles. When there is a higher

roll moment on the front axle, it results in understeer, while a higher roll moment on the rear axle leads to oversteer.

The relationship between wheel loads and the lateral force as well as the roll angle can be determined by using the sum of forces on the axle. The lateral load transfer of the vehicle can be described using the following equation derived by Gillespie (1992) and shown in Figure 2.8:

$$F_{zo} - F_{zi} = 2F_y \frac{h_r}{t} + 2K_\varphi \frac{\varphi}{t} \tag{2.15}$$

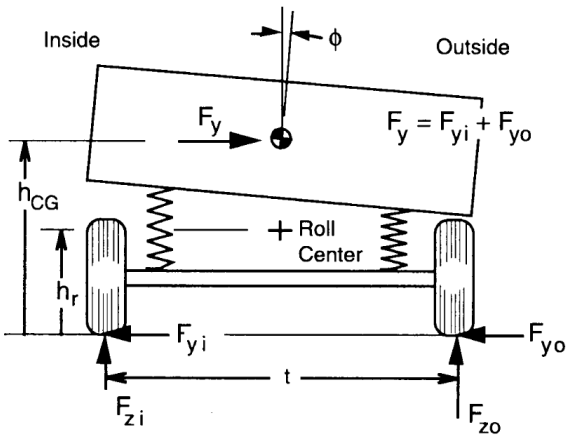

Figure 2.8. Force Analysis of a Simple Vehicle in Cornering [*Gillespie (1992)*]

We can see that the lateral load transfer stems from two mechanisms/parts of Equation 2.15. The first part of Equation 2.15 $\left(2F_y \frac{h_r}{t}\right)$ describes the lateral load transfer due to the cornering forces. This mechanism results from the lateral force applied to the axle, making it an instantaneous effect. It is independent of the body's roll angle and the roll moment distribution. The second part of Equation 2.15 $\left(2K_\varphi \frac{\varphi}{t}\right)$ describes the lateral load transfer due to the vehicle roll. The effect is influenced by roll dynamics, which may cause it to lag behind changes in cornering conditions. It is directly dependent on the distribution of the roll moment between the front and rear.

To describe the roll moment distribution further, a roll axis can be defined between the from and rear suspensions, shown in Figure 2.9:

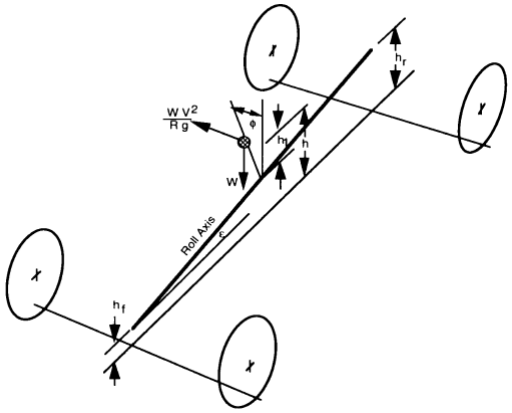

Figure 2.9. Force Analysis for Roll of a Vehicle [*Gillespie (1992)*]

The expressions for the roll moments at the front and rear axles are derived from Gillespie (1992) as:

$$M'_{\varphi f} = K_{\varphi f}\frac{Wh_1V^2/(Rg)}{K_{\varphi f}+K_{\varphi r}-Wh_1} + W_f h_f V^2/(Rg) = \Delta F_{zf} t_f \tag{2.16}$$

$$M'_{\varphi r} = K_{\varphi r}\frac{Wh_1V^2/(Rg)}{K_{\varphi f}+K_{\varphi r}-Wh_1} + W_r h_r V^2/(Rg) = \Delta F_{zr} t_r \tag{2.17}$$

The lateral load transfer is apparent in Equations 2.16 and 2.17. To relate the lateral load transfer to the effect it has on the understeer gradient, the cornering force of the tyres must relate to the slip angle and load since the slip angle on each axle will change when the load transfer is taken into account. The cornering stiffness sensitivity of a tyre can be represented by the following formula:

$$\mathrm{F_y}' = \mathrm{C}'_\alpha \alpha = \left(a\,\mathrm{F_Z} - b\,\mathrm{F_z^2}\right)\alpha \tag{2.18}$$

where a and b are coefficients in the cornering stiffness polynomial. This polynomial can be determined by fitting a second order polynomial to the tyre data obtained from the Magic Formula developed by Pacejka & Bakker (1992) or fitting a second order polynomial through experimental tyre data where cornering stiffness is determined at various vertical loads. This process is shown in Figure 2.10:

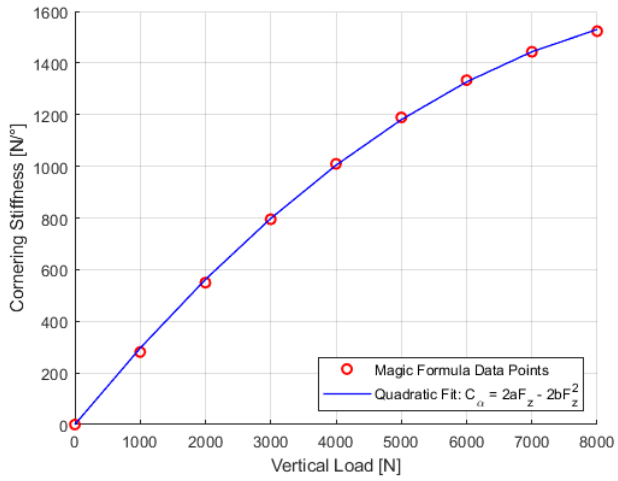

Figure 2.10. Second-order Polynomial Fit of Cornering Stiffness Sensitivity to Vertical Load

After some reduction and simplification, the steer angle for a steady-state cornering vehicle can be written as:

$$\delta = 57.3\frac{L}{R} + \left[\left(\frac{W_f}{C_{\alpha f}} - \frac{W_r}{C_{\alpha r}}\right) + \left(\frac{W_f 2b\Delta F_{zf}^2}{C_{\alpha f}^2} - \frac{W_r 2b\Delta F_{zr}^2}{C_{\alpha r}^2}\right)\right]\frac{V^2}{Rg} \tag{2.19}$$

The first term in the square brackets represents the understeer gradient arising from the cornering stiffness of the tyres, K_{tyres}. The second term is the understeer gradient defined by the lateral load transfer on the tyres of the vehicle:

$$K_{LLT} = \frac{W_f 2b\Delta F_{zf}^2}{C_{\alpha f}^2} - \frac{W_r 2b\Delta F_{zr}^2}{C_{\alpha r}^2} \tag{2.20}$$

Equation 2.19 shows that the contribution from the front axle will always result in an understeer effect as it makes the understeer gradient positive and the contribution from the rear axle will result in an oversteer effect as this makes the understeer gradient negative. The load transfer ratio between the front and rear of a vehicle often undergoes changes depending on the vehicle's steering characteristics, specifically understeer and oversteer.

Understeer typically leads to a larger load transfer on the front axle, causing the rear axle to carry less of the lateral load. Conversely, oversteer tends to result in more load transfer to the rear axle, thereby reducing the lateral load on the front axle. These variations in load transfer between the front and rear axles are significant indicators of the vehicle's handling behaviour and can influence its overall stability during different driving manoeuvres. Typically, an anti-roll bar is fitted to the axle that experiences increased load transfer during cornering to help minimise body roll and enhance the vehicle's stability.

Therefore, if the vehicle exhibits understeer tendencies (more load transfer on the front axle), installing a stiffer anti-roll bar on the rear axle can help reduce body roll and potentially mitigate understeer characteristics. Conversely, if the vehicle displays oversteer tendencies (more load transfer on the rear axle), fitting a stiffer anti-roll bar on the front axle could aid in decreasing body roll and potentially address oversteer issues.

2.2.3 Testing of Steady-State Handling

To provide objective results and repeatable experiments, simulation can be used, which also minimises the effects of driver variability. A constant radius test can be used to investigate the steady-state handling characteristics of a vehicle. These results can be used to determine the understeer gradient and can be analysed to understand how the load transfer and cornering stiffness will affect the steady-state handling characteristics. Additionally, Dukkipati (2010) states that the swept steer test also determines steering sensitivity, sideslip at the wheels, and overall compliance in the steering and suspension system during a steady-state manoeuvre.

The SAE Standard J226 (2018) states that there are five test methods to measure and determine understeer:

- Constant Radius Test
- Constant Steering Angle / Variable Speed Test
- Constant Speed / Variable Radius Test
- Constant Speed / Variable Steering-Wheel Angle Test
- Yaw Velocity Gain/Speed Test

The various testing conditions according to ISO4138 (International Organization for Standardization (2012)) are shown in Table 2.1.

Table 2.1. Steady-state Testing Conditions [International Organization for Standardization (2012)]

Test method	Constant	Varied	Measured or calculated
Constant radius	Radius	Speed	Steering-wheel angle
Constant steering-wheel angle	Steering-wheel angle	Speed	Radius
Constant speed with discrete turn radii	Speed	Radius	Steering-wheel angle
Constant speed with discrete steering-wheel angles	Speed	Steering-wheel angle	Radius

Because the understeer gradient usually quantifies the steady-state cornering characteristics of a vehicle, the methods to measure the understeer gradient experimentally will be discussed. Methods for experimental measurement of understeer gradient are based on the gradient shown in Equation 2.8. Assuming steady-state conditions, the equation is derived, and understeer defined as a characteristic specific to steady-state conditions. To experimentally measure the value of K, the vehicle needs to be manoeuvred into a steady-state turn while accurately measuring the relevant quantities mentioned in the equation above.

2.2.3.1 Constant Radius Test/Turn

During this test, the vehicle follows a circular path of constant radius, gradually increasing its speed until it can no longer maintain the path. The vehicle's lateral acceleration, yaw rate, roll angle, and various parameters, are measured during the test to assess the handling performance. The test will give insight into the oversteer and understeer characteristics of the vehicle. The curve of the steering angle versus the lateral acceleration is plotted, and the understeer coefficient is obtained with Equation 2.21:

$$\frac{\partial \delta}{\partial (\frac{a_y}{g})} = K \tag{2.21}$$

Figure 2.11 illustrates typical CRT results. If the steering angle required to maintain the vehicle on the constant radius turn is the same throughout the manoeuvre, the vehicle steers neutrally. If the slope is positive, the vehicle is experiencing understeer; if the slope is negative, the vehicle is experiencing oversteer. For actual vehicles, the value of the understeer varies with the operating condition due to tyre non-linearity, suspension effects, and load transfer. Certain vehicles exhibit consistent understeer throughout their entire operating range, maintaining this characteristic even at the limit. In contrast, some vehicles initially demonstrate understeer at low lateral acceleration levels but transition to oversteer at higher lateral acceleration levels, ultimately displaying limit oversteer. The International Organization for Standardization (2012) recommends that the radius of the circular path be at least 30 m for the constant radius test, where the standard radius can be 100 m, and 40 m is the recommended lower value.

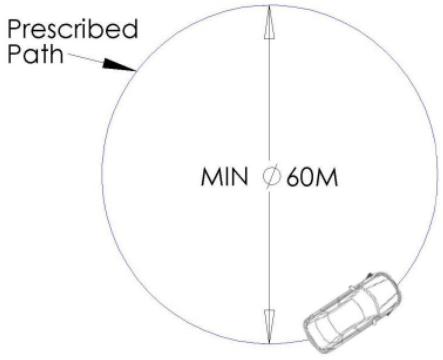

(a) Basic schematic of a constant radius handling manoeuvre [International Organization for Standardization (2012)]

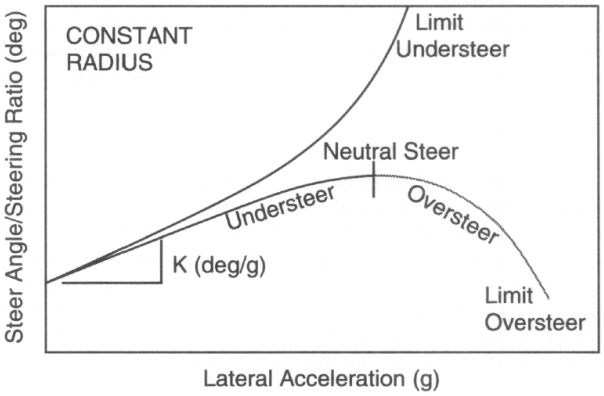

(b) Example measurements of understeer gradient by constant radius method [Gillespie (1992)]

Figure 2.11. Constant Radius Test Schematic and Example Measurements

Understeer can also be experimentally measured with the constant speed method. The speed is held constant while the steering angle is varied. This method's measurements duplicate real driving situations well as vehicles are normally driven at near constant speed.

2.2.4 Dynamic Handling

The dynamic response of a vehicle is often tested with various manoeuvres such as step steering inputs, pulse steering inputs, and double lane changes. The primary objective of these tests is to determine the transient handling response of a vehicle. Characteristic values and functions in the time and frequency domains are considered necessary for characterising vehicle transient response. [International Organization for Standardization (2011)]

2.2.4.1 Double Lane Change

The double lane change (DLC) is a standardised handling manoeuvre that has been prescribed by the ISO3888 [International Organization for Standardization (1999)] standard where it is most commonly used to evaluate the handling characteristic and vehicle dynamics of a particular vehicle with subjective emphasis. Double lane change manoeuvres can provide valuable information about the handling of a vehicle in a highly transient situation. Unlike manoeuvres such as the NHTSA Fishhook, lane changes are path-following in nature, and therefore possess an inherently high face validity. These are avoidance manoeuvres that frequently occur in the real world. This manoeuvre requires substantial driver skill.

The manoeuvre consists of two parts. First, the vehicle is driven out of its original lane into an adjacent, parallel lane, simulating an obstacle avoidance scenario. In the second part, the vehicle returns to the original lane. This manoeuvre is executed at a constant speed predetermined before the test. According to the ISO3888 standard, the manoeuvre is successfully completed if the vehicle can maintain the constant speed while staying within the defined boundaries and without knocking over any marker cones. The vehicle's performance is assessed based on the maximum speed at which it can successfully complete the manoeuvre. The test setup involves placing cones along the outer edges of the boundary lines. The layout of the double lane change is depicted in Figure 2.12.

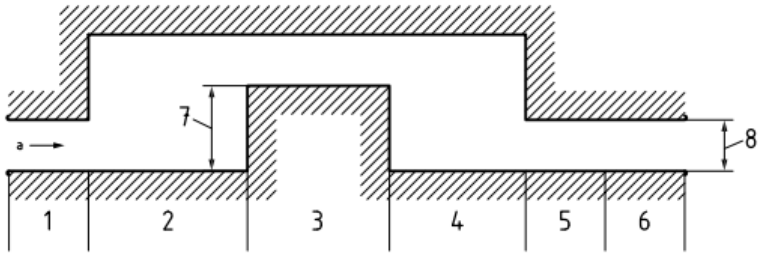

Figure 2.12. Double lane-change track and designation of sections [International Organization for Standardization (1999)]

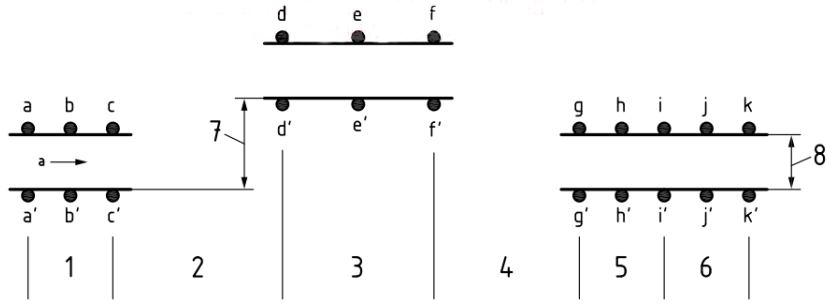

Figure 2.13. Placing of cones for marking the double lane-change track [International Organization for Standardization (1999)]

While the double-lane change manoeuvre can be seen as a method to test a vehicle's rollover propensity, Forkenbrock et al. (2004) state that tests used to measure dynamic rollover propensity may also reveal important information about handling characteristics. Other methods that test dynamic handling are the step steer manoeuvre and the step input. [Balkwill (2018)]

2.2.5 Factors Affecting Handling

2.2.5.1 Centre of Gravity Position

The distribution of passengers and/or load in road vehicles can affect the centre of gravity position, impacting handling behaviour. Automotive manufacturers implement active road-handling control strategies to address this, but vehicle mass and positioning directly influence handling. [Gillespie (1992)] Real-time monitoring of the centre of gravity is crucial for safe operation, with applications in electronic brake distribution, anti-lock braking, traction control, and rollover risk calculation. Elevated centre of gravity height increases rollover risks, while the distance between the centre of mass and roll/pitch centre impacts load transfer during acceleration. Understanding mass height relative to roll/pitch centre is crucial in SUVs and off-road vehicles. [Botha & Els (2019)] Extensive research has been conducted in the realm of vehicle load and CG estimation. Studies revealed that crucial factors influencing vehicle rollover include its mass and CG height, both estimable through various methods. Some methods, such as those based on vehicle longitudinal dynamics, do not rely on suspension or inertia parameters or lateral excitation to estimate these vital factors. [Vahidi et al. (2005), Wittmer et al. (2023)]

On the contrary, various methods exist for estimating the CG height using vehicle roll dynamics. For instance, Sanghyun et al. (2015) utilises a dual unscented Kalman Filter (UKF) to estimate the mass,

yaw moment of inertia, and longitudinal CG position through lateral and roll dynamics. Their approach incorporates a switching strategy for the UKF, validated through both simulation and experimental results. Similarly, Wang et al. (2021) introduces an adaptive Extended Kalman Filter (EKF) for roll angle and roll rate estimation based on a vehicle roll model with nonlinear suspension characteristics. COG height estimation is performed using Recursive Least Squares (RLS), albeit solely through simulation.

2.2.5.2 Suspension Effects

Hac (2002) notes that vertical "jacking" forces affect the vehicle's body during cornering on smooth roads, potentially lifting its centre of gravity above its static position. These forces originate mainly from two sources in steady-state cornering: non-linear suspension stiffness characteristics and vertical forces transmitted by suspension links. Suspension stiffness usually exhibits a progressive behaviour, increasing as the suspension deflects to maintain ride quality, even under full load. This progressive characteristic allows for minor compression deflection in the outside suspension compared to the extension deflection in the inside suspension during cornering, resulting in an elevated centre of gravity. This effect's magnitude depends on the specific suspension stiffness.

2.2.5.3 Roll Centre Height

Roll centre height refers to the theoretical point around which a vehicle's body rolls when subjected to lateral forces during cornering. It is a key parameter that influences the vehicle's stability and handling characteristics. The roll centre height significantly influences vehicle dynamics in two primary ways. Initially, it governs the alteration in tread with wheel stroke, directly impacting the tyre slip angle. When the roll centre height exceeds the ground surface, the tyre's contact point with the road shifts outward during turns. Secondly, the roll centre height plays a pivotal role in determining the vehicle's roll angle and the degree of jack-up quantity. Higher roll centre heights tend to reduce the roll angle while increasing the jack-up quantity. [Sakai & Satoh (1994)]

Widner & Bári (2018) investigated the effect of adjusting the roll centre height on the vehicle behaviour at the grip limit. All the simulations were carried out with a standard front wheel drive passenger car – defined in IPG Carmaker as an example car. The only parameter that was changed is the roll centre height of the front MacPherson suspension by lifting or lowering the inner pick-up point of the wishbone. The tests used to evaluate the change were a constant velocity turn of 100 m radius, and a straight run at constant velocity where the toe angle of the front tyres was setup to be toe in and toe out. Widner & Bári (2018) concluded that the distribution of weight transfer between front and rear axle is

proportional with the roll stiffness of the given axis. Roll centre height influences the roll stiffness. The higher the roll centre, the larger the roll stiffness of the given axis.

2.2.6 Conclusion

Data & Frigerio (2002) highlight that meaningful and objective assessments of vehicle handling characteristics can be obtained by comparing subjective evaluations from drivers during steady-state circular tests, step steering wheel inputs, and double lane change manoeuvres with objective parameters. Based on their analysis, they propose the following objective parameters as indicative of vehicle behaviour, shown in Table 2.2.

Table 2.2. Objective Indications of Vehicle Handling (Data & Frigerio (2002))

	Steering Wheel Angle	**Lateral Acceleration**	**Yaw Velocity**
Lateral Acceleration	✓		✓
Yaw Velocity	✓		
Roll Angle		✓	
Sideslip Angle	✓		

In this study, the constant radius test will be used to evaluate the steady-state handling performance of the vehicle as the effect of the lateral load transfer will lead to changes in the understeer gradient characteristic of the vehicle as well as differences in the sideslip angle will be observed. To observe the dynamic handling performance of the vehicle, the double lane change will be used as this will give insight on how the influence of lateral load transfer will effect the rollover propensity of the vehicle as well as the handling through the manoeuvre.

2.3 Rollover

Vehicle rollover is a critical event where the vehicle rotates over 90 degrees around its longitudinal axis, making contact with the ground. This can be classified into tripped and untripped rollovers. Tripped rollovers result from external factors like impacts with curbs, potholes, or guardrails. Untripped rollovers occur during cornering manoeuvres due to the interaction between lateral forces on the tyres and lateral acceleration at the vehicle's centre of gravity. Vehicles with higher centres of gravity are more prone to rollovers. Strategies to mitigate this include reducing lateral tyre forces, lowering the centre of gravity, or decreasing centrifugal force. This study delves explicitly into untripped rollovers.

2.3.1 Detection

The following section will discuss rollover detection methods, highlighting the shortcomings and advantages of each.

The load transfer ratio (LTR) is defined as the ratio of the difference between the sum of the inside wheel loads and the sum of the outside wheel loads, to the sum of all wheel loads, shown below, with reference to Figure 2.8:

$$\text{LTR} = \frac{\Sigma F_{zi} - \Sigma F_{zo}}{\Sigma F_z} \tag{2.22}$$

The LTR shows how close the vehicle is to experiencing rollover and defines *rollover* as the instant when a wheel on the vehicle experiences lift off from the ground, or when $F_z = 0$. However, Zhang et al. (2017) also confirm that the LTR is only an instantaneous piece of information without any predictive or future information available. Furthermore, Larish et al. (2013) states that the LTR is based on vehicle dynamics in terms of the detection of load transfer due to lateral acceleration. Therefore, there is difficulty in identifying a suitable LTR threshold due to external disturbances and changes.

Another method to quantify rollover is the Static Stability Factor. With reference to the nomenclature in Figure 2.8, it is defined as:

$$\text{SSF} = \frac{t}{2h_{CG}} \tag{2.23}$$

The SSF is the vehicle's at-rest calculation of its rollover resistance based on its geometric properties, highlighting how top-heavy the vehicle is. The use of the SSF to predict and characterise rollover has been criticised. An identified shortfall of the SSF is that it ignores all higher-order effects, particularly the effects of suspension and tyre compliance. Hac (2002) finds this a significant observation since the vehicle suspension allows for significant movement of wheels relative to the body, resulting in changes in half-track width and position of the vehicle centre of gravity during large lateral accelerations.

Lapapong et al. (2012) propose the zero moment point (ZMP) as an alternative to the SSF and the LTR methods, based on the contact point of the vehicle relative to the edge of the support polygon without requiring the tyre forces or being based on steady-state behaviour. The ZMP is the point on the ground where the summation of the tipping moments acting on an object due to gravity and inertial forces, is equal to zero. If the net force vector of the object to the ground acts within the contact polygon of the object to the ground, the object will remain in dynamic equilibrium.

The ZMP's proximity to the edge of the support polygon is considered the dynamic metric to evaluate the vehicle's rollover propensity. Therefore, if the ZMP's lateral position is outside the vehicle's track width, the vehicle will become unstable and experience wheel lift. The ZMP's distance relative to the vehicle's centre line is known as y_{ZMP}.

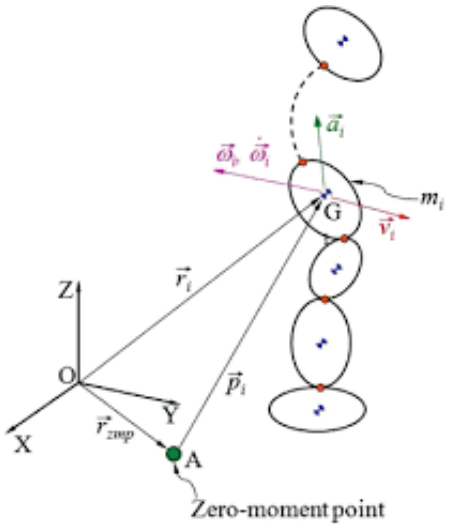

Figure 2.14. Kinematic Chain of Bodies Lapapong et al. (2012)

Larish et al. (2013) propose a predictive load transfer ratio (PLTR) that improves on the traditional load transfer ratio discussed in Section 2.2.1.1. The traditional LTR only considers a snapshot of the instantaneous vehicle dynamics. while the PLTR utilises a driver's steering input and several other sensor signals available from the vehicle's electronic stability control system. Larish et al. (2013) then discuss the advantages of the new PLTR over the typical LTR; it can act as part of a warning system to predict rollover rather than detection. Also, it is easier to set the activation threshold since the trade-off between false alarms and safety is reduced due to the increased time available for preventative action. Another advantage is that more vehicle information is used in the index, and inexpensive sensors can easily measure all required feedback variables. The last advantage stated is that the new PLTR can be used in rollover prevention systems, including torque management or brake-based stability control systems and suspension control.

Tian et al. (2018) propose an advanced method aimed at predicting the tendency of the lateral load transfer ratio (LTR), a key indicator for rollover risks. The objective is to offer ample lead time for the control system to optimise its response. Initially, an estimation equation was proposed to enhance LTR estimation accuracy, validated using Simulink and TruckSim. To enhance practicality, a buffer operator was integrated to mitigate drawbacks. Simulation outcomes demonstrated the efficacy of the grey LTR (GLTR) in accurately predicting LTR trends based on current and past data. During Sine with Dwell and double lane change tests, the GLTR effectively provided the control system with preparatory time. Moreover, a differential system model validated the GLTR's performance, showcasing its potential to enhance rollover prevention systems by delivering anticipated responses during the Sine with Dwell manoeuvre.

2.3.2 Testing/Measuring of Rollover Propensity

2.3.2.1 Fishhook Test

One method for assessing a vehicle's rollover risk is the Fishhook manoeuvre, regarded as one of the most severe tests by the National Highway Traffic Safety Administration (NHTSA) for untripped rollover propensity. As demonstrated by Forkenbrock et al. (2004), this test involves driving the vehicle slightly above the desired entrance speed in a straight line and then initiating steering commands using a steering robot. The steering inputs are initially 6.5 times the steering input required for 0.3 g lateral acceleration at 80 km/h. After a dwell time, a counter-steer input is applied. The test parameters are determined through a Slowly Increasing Steer test, with its results informing the Fishhook test. This comprehensive evaluation is performed at various entrance speeds until a two-wheel lift exceeding 50.8 mm occurs simultaneously. Figure 2.15 illustrates the steering wheel angle input and the manoeuvre schematic for the Fishhook Test:

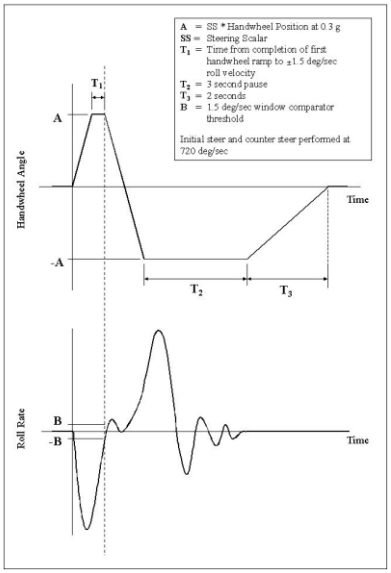

(a) NHTSA Fishhook Manoeuvre Steering Wheel Angle Description [Forkenbrock et al. (2004)]

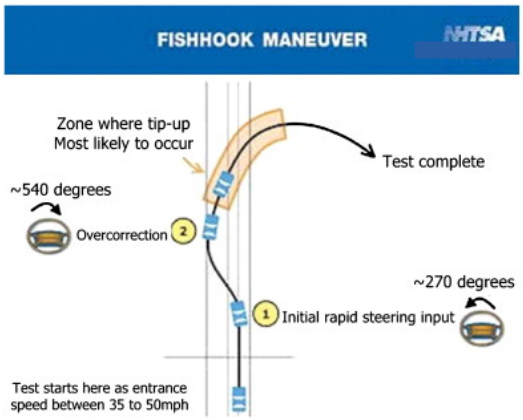

(b) NHTSA Fishhook Manoeuvre Schematic [Yoon et al. (2010)]

Figure 2.15. NHTSA Fishhook Test Procedure

2.3.2.2 NHTSA J-Turn

The NHTSA Fishhook 1b was found to be the most objective and repeatable of all the rollover resistance manoeuvres performed during Phase IV of the NHTSA Rollover Research Phases by Forkenbrock et al. (2004). This is due to the ease of inputting the steering wheel angle required by using a programmable steering machine. Additionally, the variables and states investigated (vehicle speed, lateral acceleration, and roll angle) were observed to be highly repeatable. The comparison between the manoeuvres performed by the NHTSA is shown in Table 2.3:

Table 2.3. NHTSA Summary of Rollover Resistance Manoeuvre Scores [Forkenbrock et al. (2003)]

Assessment Criterion	NHTSA J-Turn	Fishhook 1a	Fishhook 1b	Nissan Fishhook
Objectivity and Repeatability	Excellent	Excellent	Excellent	Good
Performability	Excellent	Good	Excellent	Satisfactory
Discriminatory Capability	Excellent[1]	Excellent	Excellent	Excellent
Appearance of Reality	Good	Excellent	Excellent	Good

The NHTSA J-Turn was derived from the J-Turn used during NHTSA's Phase II rollover research program. However, the steering wheel magnitudes were calculated by multiplying the steering wheel angle that produced an average of 0.3 g in the Slowly Increasing Steer manoeuvre by a scalar of 8.0. The rate of the steering wheel angle ramp was 1000 degrees per second. The J-Turn manoeuvre uses automated steering inputs commanded by a programmable steering robot. [Forkenbrock et al. (2003)]

[1] When limited to vehicles with low rollover resistance and/or disadvantageous load configurations.

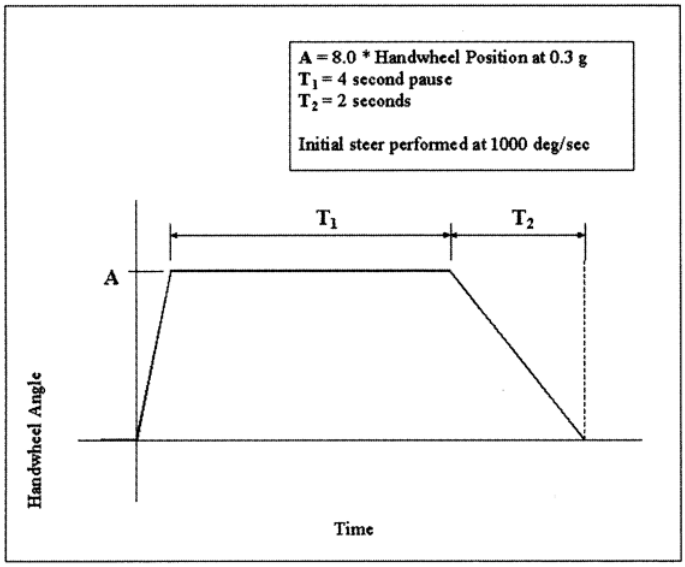

Figure 2.16. NHTSA J-Turn Steering Wheel Angle Input [Forkenbrock et al. (2003)]

To begin the manoeuvre, the vehicle is driven in a straight line at a speed slightly higher than the desired entrance speed. The driver releases the throttle, coasts to the target speed, and triggers the commanded steering wheel input described in Figure 2.16. The nominal manoeuvre entrance speeds used in the J-Turn manoeuvre range from 35 to 60 miles per hour (56 to 97 km/h) and increased in 5 mile per hour (8 km/h) increments until a termination condition is achieved. Termination conditions include a two-wheel lift or completion of a test performed at the maximum manoeuvre entrance speed without a two-wheel lift. If a two-wheel lift is observed, a downward iteration of vehicle speed is used in 1 mph increments until such lift is no longer detected. Once the lowest speed for which a two-wheel lift could be detected is isolated, two additional tests were performed to monitor repeatability.

2.3.3 Conclusion

In this section, an exhaustive analysis encompassing studies aimed at detecting and evaluating the propensity of rollover risk in vehicles was conducted. Through an in-depth exploration, valuable insights were extracted, delving into a spectrum of testing methodologies. It has been determined that the Fishhook 1b test will be the primary evaluation tool employed within this thesis to assess the potential for rollover.

2.4 Methods to Improve Handling Characteristics and Rollover Mitigation using Suspension Control

The preceding sections discussed and investigated factors that influence handling and rollover. It is evident that there are various methods of improving the handling characteristics and reducing the rollover propensity of a vehicle, including making changes to the vehicle's physical dimensions (track width, ride height, etc.) or the aerodynamics of the vehicle. In this report, we will focus on methods that can be controlled using software and hardware as well as those that do not require arduous amounts of effort to alter since most of the dimensions on a vehicle are constrained and cannot be changed with ease. Table 2.4 illustrates the differences between automotive suspensions:

Table 2.4. Comparisons between various automotive suspension [Liu et al. (2014)]

Parameters	Passive Suspensions	Semi-active Suspensions	Hydraulic or Pneumatic Active Suspensions	Electromagnetic Active Suspensions
Structure	Simplest	Complex	Most complex	Simple
Weight/Volume	Lowest	Low	High	Highest
Cost	Lowest	Low	Highest	High
Ride comfort	Bad	Medium	Good	Best
Handling performance	Bad	Medium	Good	Best
Reliability	Highest	High	Medium	High
Dynamic performance	Passive	Passive	Medium	Good
Energy regeneration	No	No	No	Yes
Commercial maturity	Yes	Yes	Yes	No

2.4.1 Semi-Active Suspensions

Active suspensions adjust themselves continuously to counter the changing road conditions by adjusting mechanical connections between the chassis and wheel assemblies to absorb the energy caused by the vertical motion of the wheels. **Active suspensions** require significant amounts of energy to operate, leading to highly complex systems and an increase in the overall size of the suspension package. **Semi-active suspensions** are systems that can adjust the viscous damping coefficient of the damper and the spring rate.

Therefore, these systems use methods such as altering electric current through a ferrous fluid, and electronically controlled valves that adjust the flow of hydraulic fluid in the strut to alter the damping characteristics.

Semi-active control mechanisms present a level of dependability comparable to that of passive devices while maintaining the adaptability and versatility of fully active systems. Furthermore, these systems do not necessitate large power sources. In a **semi-active suspension**, the amount of damping can be adjusted, whereby most devices modulate the damping forces according to the implemented control strategy. In contrast to active control devices, semi-active control mechanisms cannot inject mechanical energy into the regulated system, thus avoiding destabilising it. Examples of such devices include variable orifice dampers, controllable friction devices, and dampers with controllable fluids, such as magnetorheological and electrorheological fluids. [Guglielmino et al. (2008)]

Isermann (2022) states that load-levelling systems can typically serve a semi-active purpose, provided they offer the necessary control dynamics. A typical semi-active spring configuration relies on either an air spring or a hydropneumatic system. The stiffness of an air spring can be estimated using the equation proposed by Reimpell & Stoll (1996), as follows:

$$c = n\frac{pA^2}{V} \tag{2.24}$$

Consequently, pneumatic systems adjust the air volume V by adding or removing air, thereby altering stiffness, enabling a continuously adjustable stiffness.

Ahmadian & Simon (2004) conducted an experimental study in which they implemented and evaluated the effectiveness of Skyhook control and steering input augmented (SIA) skyhook control on a 2000 Ford Expedition SUV. The vehicle was equipped with magneto-rheological semi-active dampers to control the suspension damping. The swerve test was selected as the manoeuvre for evaluation, involving driving the vehicle in a straight line, performing a swerve manoeuvre to avoid an obstacle, and then returning to the original lane. The swerve test was conducted at a speed of 20 mph (33 km/h), and the pitch and roll acceleration were utilised as quantitative measures during the test. The findings indicated that the Skyhook control and SIA skyhook control systems demonstrated a notable improvement of more than 10% in reducing roll and pitch acceleration compared to the standard passive suspension system. The SIA control, however, provided only a small reduction in suspension travel, as compared to other suspensions that were tested.

Lee et al. (2021) proposed a simplified approach for controlling magneto-rheological (MR) dampers by estimating damper velocity and reducing the number of required accelerometers. They utilised an inertial measurement unit (IMU) sensor on the sprung mass to calculate acceleration at each damper's top, factoring in its specific mounting axis. This estimated damper velocity was then compared with the lower damper's measured acceleration and integrated into the semi-active suspension controller via the CAN bus. Validation was performed through a mid-sized SUV model simulation, with the vehicle model and algorithm co-simulated at a 5 ms communication interval. A 60-second simulation on a random road profile at 60 km/h on a C-class road surface was conducted to verify accuracy. Results showed that the state estimator closely matched damper speed for passive vehicles and yielded no differences in damping forces for semi-active suspension vehicles with MR dampers.

Van Der Sande et al. (2022) devised a rule-based controller for a semi-active suspension system, aiming to bolster road-holding performance. It evaluates effectiveness by analysing tyre deflection at each wheel—the control rule factors in unsprung mass, suspension deflection velocity, and excitation frequency for efficient switching. The proposed controller significantly minimises tyre deformation across the frequency range compared to passive and existing semi-active configurations. Experimental tests focus on unsprung mass acceleration due to practical constraints in measuring tyre deflection. Results show up to an 11% reduction in RMS unsprung acceleration compared to the best-performing passive configuration, following a predetermined trajectory.

The Ford GT utilises a sophisticated suspension system with two springs per wheel designed by Multimatic Inc. (2023), active in Normal mode and featuring firmer DSSV dampers in Sport mode. High-performance settings lock out one spring, doubling the spring rate and lowering the ride height. Audi's Adaptive Air Suspension system enhances handling and ride comfort, autonomously adjusting ride height and including load-dependent level control. The system's design varies by model, with air springs integrated into front struts and separately in most rear suspensions. BMW employs the Adaptive BMW M Suspension with electromagnetically controlled valves for continuous damping adjustment, allowing for comfort on rough roads and firm handling for high-speed driving. [BMW M (2023)]

Els (2006) stated that the design of vehicle suspension systems always involves a compromise between ride comfort and handling where ride comfort will require a soft suspension to minimise the road input disturbances carried through to the occupants and optimal handling will require a stiff suspension to minimise the body roll angle of the vehicle. By achieving a controllable suspension, the suspension characteristics can be altered while the vehicle is in motion, possibly eliminating the compromise between ride comfort and handling. Els (2006) conducted a full-vehicle model simulation and deduced that at least two discrete spring and damper characteristics were required to eliminate and address the ride comfort and handling compromise. The handling suspension configuration included a stiff spring and high damping, whereas the ride comfort suspension configuration included a soft spring and low damping. The suspension system was named the 4-State Semi-Active Suspension System as it is capable of combining the two spring characteristics and damping characteristics to give four states.

The implementation of continuous variable damping was the following addition to the system developed by Els (2006) and the system was named the $4S_4$CVD. The system consists of two solenoid flow-control valves which can restrict and block flow through the valve to achieve increased damping as well as a higher stiffness. In addition to the two new solenoid valves, two valves are implemented into the system which will allow for ride height control to be achieved. The $4S_4$CVD was characterised, modelled and tested by Vosloo (2019). The design of the $4S_4$CVD is shown in Figure 2.17:

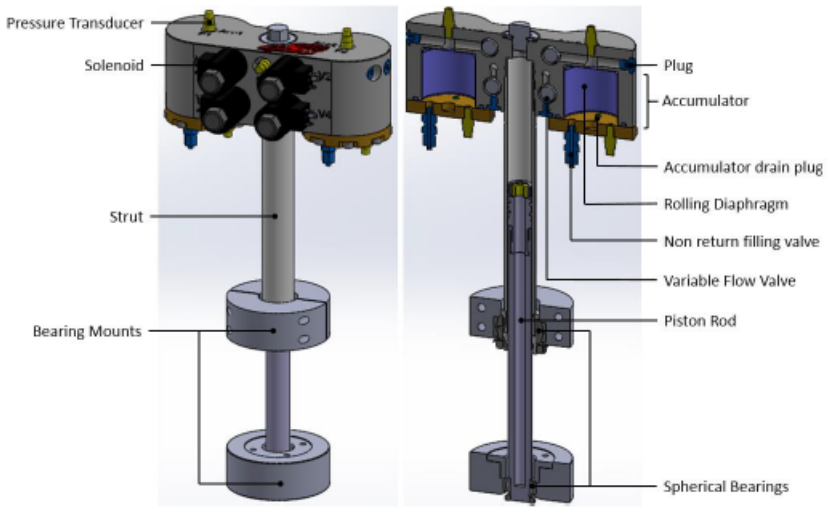

Figure 2.17. $4S_4$CVD CAD Design [*Vosloo (2019)*]

Another change made to the initial $4S_4$ include a reduction in the piston diameter, which allows for a smaller package as well as achieving lower damping due to the reduction of the induced flow rate induced by the piston movement. The characterisation and modelling of the $4S_4$CVD were done extensively by Vosloo (2019) where the damping characteristics of the new solenoid valves were capable of achieving a significantly lower damping setting than the $4S_4$ developed by Els (2006), which had a higher than optimal characteristic required for ride comfort. Figure 2.18 indicates the spring and damper characteristics for the $4S_4$CVD:

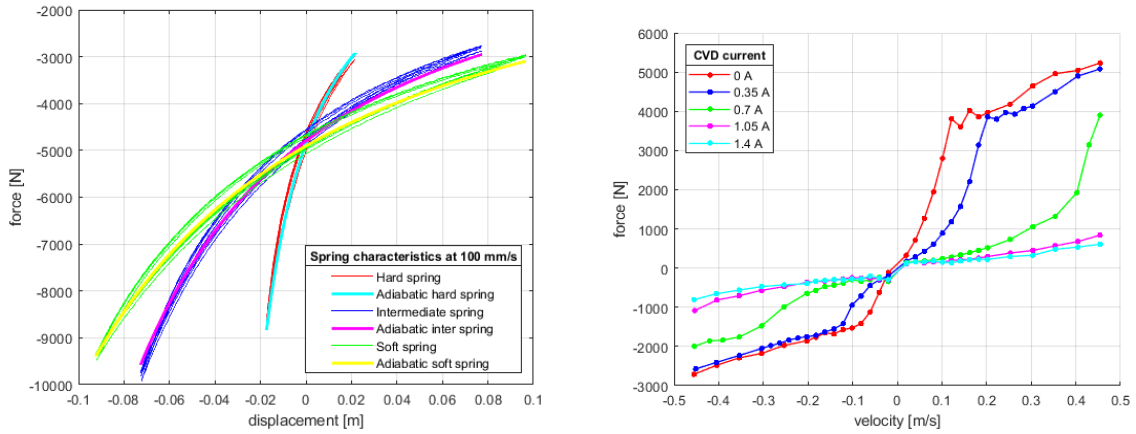

(a) $4S_4$CVD force versus displacement spring characteristics with bulk modulus compensation

(b) $4S_4$CVD full damping envelope of prototype considered during experimental testing

Figure 2.18. Spring & Damping Characteristics of the $4S_4$CVD

Vosloo (2019) concluded that sufficient variable damping is achievable through the use of the solenoid valves. De Wet (2020) proposed that the architecture presented by Vosloo (2019) faced feasibility challenges. These arose from an inherent issue wherein the valve's closed position resulted in a suspension system lock-up. This occurred due to the substantial non-linearity when nearing the closed position, leading to an escalation in damping force to infinity. The proposed solution was the addition of a blow-off damper placed in parallel to the proportional flow control valve, which provides the required high damping for optimal handling when the proportional flow control valve is closed.

As a result, the optimal handling characteristic in addition to a low characteristic optimal for ride comfort with variability between the two states could be achieved. The region for active controllability will be advised to be in the 0.3A - 1A range while using the fully open and fully closed setting for extreme handling and ride comfort cases.

2.4.2 Anti-Roll Implementations

Various strategies aim to reduce vehicle rollover risk. Electronic Stability Control (ESC) systems, using sensors to monitor vehicle dynamics like steering input, yaw rate, and lateral acceleration, selectively apply brakes and reduce engine power to maintain stability during critical situations. [S. Minjun & Kanghyun (2018)] Active roll control systems use hydraulic actuators or adjustable anti-roll bars to counteract body roll during cornering, enhancing stability and reducing rollover risk. [Yu et al. (2008), Kim & Huh (2019)] Active suspension systems, like adaptive dampers or air suspensions, continuously adjust damping and ride height based on conditions and vehicle dynamics, improving stability, reducing body roll, and enhancing handling, thus reducing rollover risk.

2.4.2.1 Active Anti-Roll Bars

Anti-roll bars play a crucial role in controlling the roll stiffness of a vehicle, decoupled from its vertical (ride) stiffness. By independently adjusting the roll stiffness, anti-roll bars can regulate the vehicle's body roll angle and manage the distribution of vertical load between the left and right wheels. Active anti-roll bars, comprising an anti-roll bar and an actuator, enhance the effectiveness of passive anti-roll bars by enabling them to act selectively when required, optimising their impact on the vehicle's dynamics.

Hwang et al. (2020) conducted a study on an active anti-roll bar in an electric medium-sized bus to enhance vehicle handling performance by adjusting anti-roll bar stiffness and damping to minimise roll angles. The strategy involved increasing front rolling stiffness to counteract oversteer, reducing load shift to the front outer wheel, improving front inner tyre traction, and enhancing stability. Conversely, when the vehicle experienced excessive understeer, the rear rolling stiffness was increased, enhancing rear inner tyre traction. The control process activated or deactivated the front and rear anti-roll bars based on the difference between front and rear slip angles. Simulation results showed a 54.08% reduction in stabilisation time and improved handling behaviour, making the vehicle more stable at high speeds and reducing yaw angle changes by 14.6%. Figure 2.19 illustrates the flowchart of the control logic used by Hwang et al. (2020).

Vu et al. (2016) conducted a study focusing on the design of active anti-roll bars for optimising vehicle roll stability. They employed a linear quadratic regulator (LQR) to model four electronic servo-valve hydraulic dampers on a yaw-roll model of a single-unit heavy vehicle. The aim was to limit lateral load transfer within safe levels to prevent wheel lift-off during a double lane change, achieving stability by

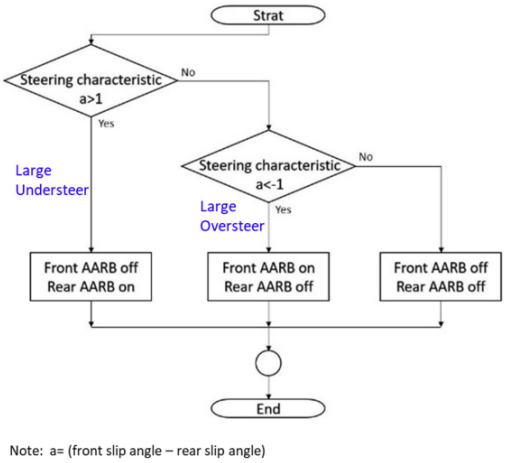

Figure 2.19. Active Anti-Roll Bar Control Strategy [Hwang et al. (2020)]

minimising load transfer and promoting inward lean. Results showed that the LQR active anti-roll bar effectively maintained lateral load transfers within safe bounds, ensuring roll stability. Both active anti-roll bar controllers significantly improved vehicle roll stability compared to scenarios without an anti-roll bar or with a passive one.

2.4.2.2 Active Suspension Control

Active suspension control systems have emerged as an advanced technology with the potential to revolutionise vehicle dynamics by offering real-time adjustments to suspension characteristics. Leveraging many sensors and actuators, active suspension control allows for manipulating critical parameters like damping forces, stiffness, and ride height. By dynamically adapting these parameters based on changing driving conditions, active suspension control can effectively counteract rollover tendencies and significantly enhance vehicle stability.

Wang & Shen (2008) presented an innovative method utilising active suspension to induce controlled vehicle tilting in response to turns. They constructed a detailed vehicle model incorporating a 6-degree-of-freedom structure with a 2-degree-of-freedom steering model and a 4-degree-of-freedom tilting model. This enabled precise determination of the desired tilt angle, leading to the development of an active tilt-sliding mode controller focused on eliminating steady-state tilt angle errors. The proposed controller demonstrated exceptional effectiveness in reducing perceived lateral acceleration and lateral load transfer rates through extensive simulations incorporating magneto-rheological dampers. This significantly improved handling stability, ride comfort, and vehicle speed. Moreover, the control strategy showed promise in reducing the likelihood of rollover incidents during dynamic turning

manoeuvres, highlighting its potential for enhancing safety and performance.

Lee et al. (2022) introduced a novel high-efficiency active suspension system based on continuous damping control (CDC). The approach optimises ride performance by selectively using the actuator for active scenarios and relying on CDC for other situations. This involves formulating both active suspension models and controllers and designing control logic to calculate actuator force based on suspension components. The system enhances energy efficiency by distinguishing between active and semi-active modes, using CDC when the force falls within the damper's control range. The actuator is engaged outside this range to improve ride performance. Evaluation under various driving conditions confirmed the system's effectiveness, identifying an ideal suspension structure for this active control system.

2.4.3 Ride Height Control

Height adjustable suspension represents a sophisticated feature embedded in specific automotive suspension systems, empowering drivers to modify the vehicle's ride height or ground clearance as needed. The versatility of this system serves multiple purposes, encompassing the provision of enhanced ground clearance to navigate rough or challenging terrains effectively. Conversely, it also enables lowering the vehicle's ground clearance, thereby potentially improving performance and fuel efficiency at higher speeds. The modification of vehicle height is accomplished by employing air or oil compression to the vehicle's springs. The adjustment is executed by varying the pressure, causing the vehicle body to ascend or descend. The suspension system can maintain the optimal ride height by adjusting to changes in load or aerodynamic forces, ensuring that it can effectively absorb shocks and bumps while eliminating any variations in handling that might occur if operated at a height other than the intended design ride height. [Gillespie (1992)]

Several studies ride height control with implemented into air suspension systems where various control strategies were implemented, such as nonlinear model predictive control [Ma et al. (2018)], variable structure control [Xu et al. (2013)], and tuning [Karimi Eskandary et al. (2016)]. These studies looked at the aspect of lowering and raising heavy vehicles in stationary positions and, therefore, did not investigate the effect of the height adjustment in dynamic situations such as undulating terrain or when performing manoeuvres.

2.5 Validated Full Non-Linear Vehicle Simulation Model

To perform the simulations required for the analysis of this thesis, ADAMS will be used to simulate a vehicle that represents a real-world scenario and accurate physics. The test vehicle for the study is a Land Rover Defender 110 fitted with the $4S_4$CVD hydro-pneumatic suspension system.

The complete model of the Land Rover used was developed by Uys et al. (2007) using the multi-body dynamics software MSC Adams [Hexagon (2023)]. The fully non-linear model contains 16 degrees of unconstrained freedom of the real vehicle and has been extensively validated as it has been the subject of numerous research projects at the Vehicle Dynamics Group at the University of Pretoria.

Table 2.5. Adams vehicle model degrees of freedom [Thoresson (2007)]

Body	Degrees of Freedom	Associated Motion
Vehicle Body (2 rigid bodies)	7	body torsion longitudinal, lateral, vertical roll, pitch, yaw
Front Axle	2	roll, vertical
Rear Axle	2	roll, vertical
Wheels	4 x 1	rotation

The load-dependent lateral and vertical tyre dynamics are considered in this model; thus, the load transfer of the vehicle during the constant radius test manoeuvre can be verified. The vehicle body has been modelled as two rigid bodies connected along the roll axis at chassis height by a revolute joint and a torsional spring. This was done to better capture the vehicle dynamics due to body torsion in roll. The model includes a validated FTire (cosin scientific software (2020)) tyre model of the Pirelli Scorpion Verde 235/55 R19 all-season tyre investigated by Wright et al. (2019). The vehicle's model parameters are shown below in Table 2.6:

Table 2.6. Land Rover Simulation Model Vehicle Parameters [Uys et al. (2006)]

Parameter	Value	Unit
Total Vehicle Mass	2047	kg
Vehicle Sprung Mass	1582	kg
Roll Mass Moment of Inertia	839	kgm^2
Pitch Mass Moment of Inertia	2471	kgm^2
Yaw Mass Moment of Inertia	2057	kgm^2
Longitudinal distance from the front axle to CG	1.55	m
Longitudinal distance from the rear axle to CG	1.25	m
Track Width	1.49	m
Distance between Front Suspension Struts	1.01	m
Distance between Rear Suspension Struts	0.97	m
Vehicle Width	1.86	m

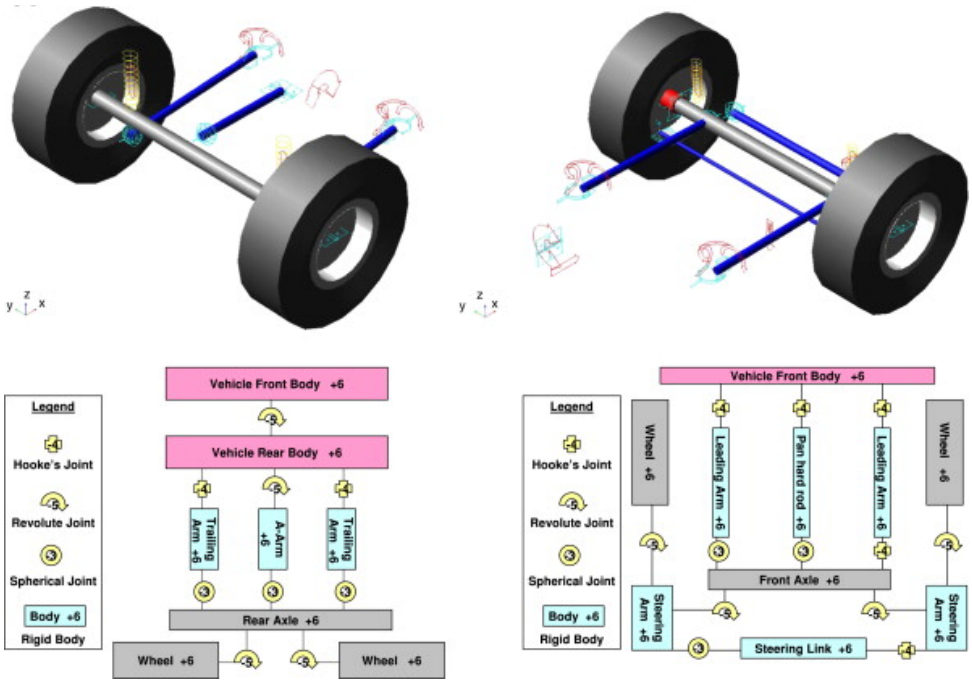

Figure 2.20. Modelling of the rear and front suspensions in MSC Adams [Thoresson (2007)]

The Adams model integrates the 4S4CVD suspension model by co-simulating it with Simulink. This suspension is connected to a solid axle, featuring vertically-mounted suspension struts. To accurately mirror real-world systems, the model incorporates non-linear bump stops, bushings, and friction. Additionally, the driver model employed is used for path following model and longitudinal demand forces previously developed by Botha (2011) and Hamersma (2013).

2.6 Conclusion

The literature review comprehensively explored the foundational vehicle dynamics that influence a vehicle's handling characteristics. Through the application of yaw-plane analysis, the impact of tyre forces on steering behaviour and the derivation of the vehicle's understeer gradient were discerned. Additionally, roll-plane analysis was to identify critical parameters affecting the roll angle's magnitude and propagation. This review also delved into the intricate effects of load transfer on understeer. A range of handling and rollover metrics were examined, with particular emphasis on roll angle and lateral acceleration, which serve as valuable indicators for evaluating the handling limits of SUVs. Notably, the study highlighted that augmenting vehicle roll stiffness and damping characteristics, primarily achieved through strategic adjustments in the suspension system, presents a promising avenue to limiting roll angle propagation, and maintain a stable understeer gradient, especially during lateral load transfer.

This literature study has created the basis to investigate the handling improvement and rollover mitigation of an off-road vehicle using the lateral load transfer of the vehicle. The research questions posed in Section 1.2 can thus be addressed as follows:

- Lateral load transfer has a significant effect on both the handling performance and rollover propensity of a vehicle.
- SUVs have higher CGs and roll arms, and hence this effect is amplified. This explains why SUVs handle worse and are more prone to rollover than conventional passenger cars.
- The literature review indicates that the suspension characteristics may significantly influence the load transfer during cornering.
- Ride height control is another promising approach to influence load transfer and lead to improved handling and lower rollover propensity.

Therefore, it is hypothesised that the suspension characteristics and ride height control may be integrated into a control system with the aim of improving handling and rollover propensity. The control system will use the vehicle's roll angle as well as the difference in the front and rear slip angles to evaluate the effectiveness of the system in mitigating rollover and improving handling performance.

3. Simulation Results & Analysis

3.1 Introduction

This chapter encompasses the analysis addressing the research query concerning the enhancement of handling performance and the reduction of rollover risks through load transfer manipulation. Initial investigation involves conducting a first-order analysis to corroborate the theories outlined in Chapter 2 and to deepen comprehension of the issue at hand. Subsequently, the ADAMS simulation platform is employed to substantiate the research query and the initial analysis. The Land Rover Defender 110, integrated with the $4S_4$CVD system referenced in section 2.3.1.1, serves as the test vehicle. Simulation exercises focus on resolving the optimal suspension configuration to achieve diverse steering characteristics, aiming to ascertain the viability of influencing load transfer. The primary objective is to identify the configuration that facilitates the most neutral steer characteristic, which will lay the groundwork for the implementation of ride height control.

3.2 First Principle Analysis

To understand the possible solution to the research question, a first principle analysis of vehicle dynamics can be used to predict what will happen when the vehicle experiences certain manoeuvres. It begins by referring to the solution for roll moments at the front and rear axles of the vehicle, stated below:

$$M'_{\phi f} = K_{\phi f}\frac{Wh_1V^2/(Rg)}{K_{\phi f}+K_{\phi r}-Wh_1} + W_f h_f V^2/(Rg) = \Delta F_{zf} t_f \tag{3.1}$$

$$M'_{\phi r} = K_{\phi r}\frac{Wh_1V^2/(Rg)}{K_{\phi f}+K_{\phi r}-Wh_1} + W_r h_r V^2/(Rg) = \Delta F_{zr} t_r \tag{3.2}$$

Since the load transfer effect is crucial in order to influence the vehicle's handling performance and rollover propensity, the load transfer can be made the subject of Equations 3.1 and 3.2:

$$\frac{K_{\phi f}\frac{Wh_1V^2/(Rg)}{K_{\phi f}+K_{\phi r}-Wh_1} + \frac{W_f h_f V^2}{Rg}}{t_f} = \Delta F_{zf} \tag{3.3}$$

$$\frac{K_{\phi r}\frac{Wh_1V^2/(Rg)}{K_{\phi f}+K_{\phi r}-Wh_1} + \frac{W_r h_r V^2}{Rg}}{t_r} = \Delta F_{zr} \tag{3.4}$$

The roll stiffness of the vehicle is is required to derive the load transfer analytically. This is defined for each axle as:

$$K_\phi = \frac{1}{2}K_s s^2 \tag{3.5}$$

where K_s is the spring rate of the suspension. With the hydropneumatic spring, the spring rate at the static position of the vehicle is calculated as follows:

$$K_s = \frac{nF_{stat}A}{V} \tag{3.6}$$

To capture the non-linearity of the hydropneumatic spring, the force in the spring is calculated in terms of a volume change of gas in the spring using the static conditions:

$$F(\Delta V) = F_{stat}\left(\frac{V_{stat}}{V_{stat}+\Delta V}\right)^n \tag{3.7}$$

Using this force, the roll stiffness of the front axle can be calculated and visualised more accurately in Figure 3.1:

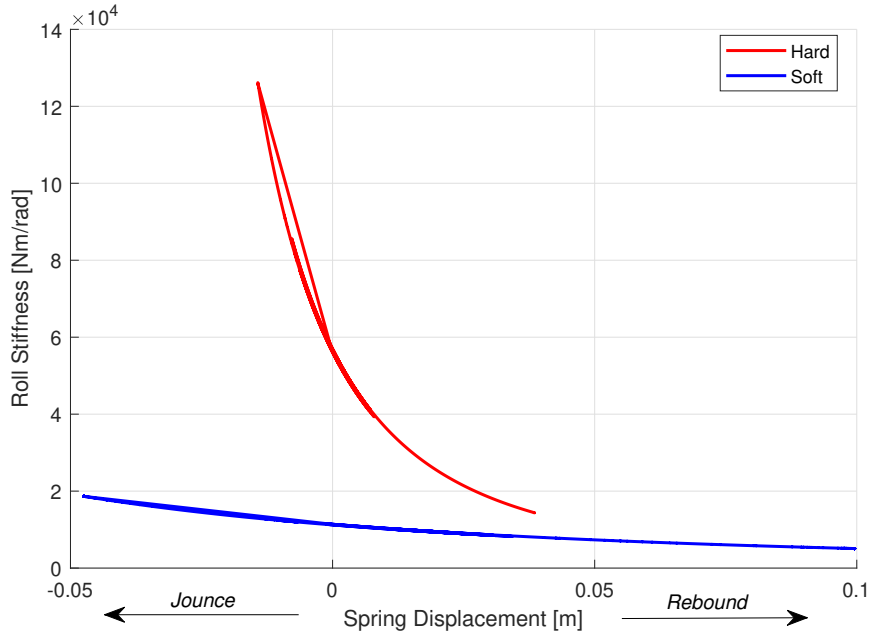

Figure 3.1. First Principle Analytical Roll Stiffness

This proves that the load transfer on a certain axle can be influenced by making it stiff or soft. Using this information, it is illustrated how the understeer characteristic of the vehicle will be affected by the change in the suspension configurations through a constant radius test by using Equation 3.8:

$$\delta = 57.3\frac{\mathrm{L}}{\mathrm{R}} + \left[\left(\frac{\mathrm{W_f}}{\mathrm{C_{\alpha f}}} - \frac{\mathrm{W_r}}{\mathrm{C_{\alpha r}}}\right) + \left(\frac{\mathrm{W_f}}{\mathrm{C_{\alpha f}}}\frac{2b\Delta\mathrm{F_{zf}^2}}{\mathrm{C_{\alpha f}}} - \frac{\mathrm{W_r}}{\mathrm{C_{\alpha r}}}\frac{2b\Delta\mathrm{F_{Zr}^2}}{\mathrm{C_{\alpha r}}}\right)\right]\frac{\mathrm{V^2}}{\mathrm{Rg}} \tag{3.8}$$

This illustrates that there is an expectation to see understeer for the vehicle in a hard-front configuration and oversteer for the rest of the suspension configurations. When investigating the calculated steering angles using tyre cornering stiffness and lateral load transfer components, this confirmation is further reinforced:

$$K_{tyres} = \left(\frac{\mathrm{W_f}}{\mathrm{C_{\alpha f}}} - \frac{\mathrm{W_r}}{\mathrm{C_{\alpha r}}}\right) \quad \text{and} \quad K_{LLT} = \left(\frac{\mathrm{W_f}}{\mathrm{C_{\alpha f}}}\frac{2b\Delta\mathrm{F_{zf}^2}}{\mathrm{C_{\alpha f}}} - \frac{\mathrm{W_r}}{\mathrm{C_{\alpha r}}}\frac{2b\Delta\mathrm{F_{Zr}^2}}{\mathrm{C_{\alpha r}}}\right) \tag{3.9}$$

Figure 3.2 provides an insightful depiction of how each constituent of the understeer gradient influences the vehicle's steering characteristics. The understeer gradient stemming from the tyre component triggers an oversteer tendency as the rear weight exceeds the front weight. Interestingly, both the fully soft and fully hard configurations exhibit similar behaviours owing to the linear attributes of the spring model. However, this conformity contradicts expectations within the nonlinear suspension model, where the hard suspension configuration should resist spring compliance as the vehicle undergoes increased rolling and encounters higher lateral acceleration. The soft front configuration experiences pronounced oversteer due to amplified load transfer at the rear, while the hard front configuration tends toward significant understeer as it encounters heightened load transfer at the vehicle's front. These distinctions underscore the varied impacts of load distribution on steering behaviour based on the suspension configuration.

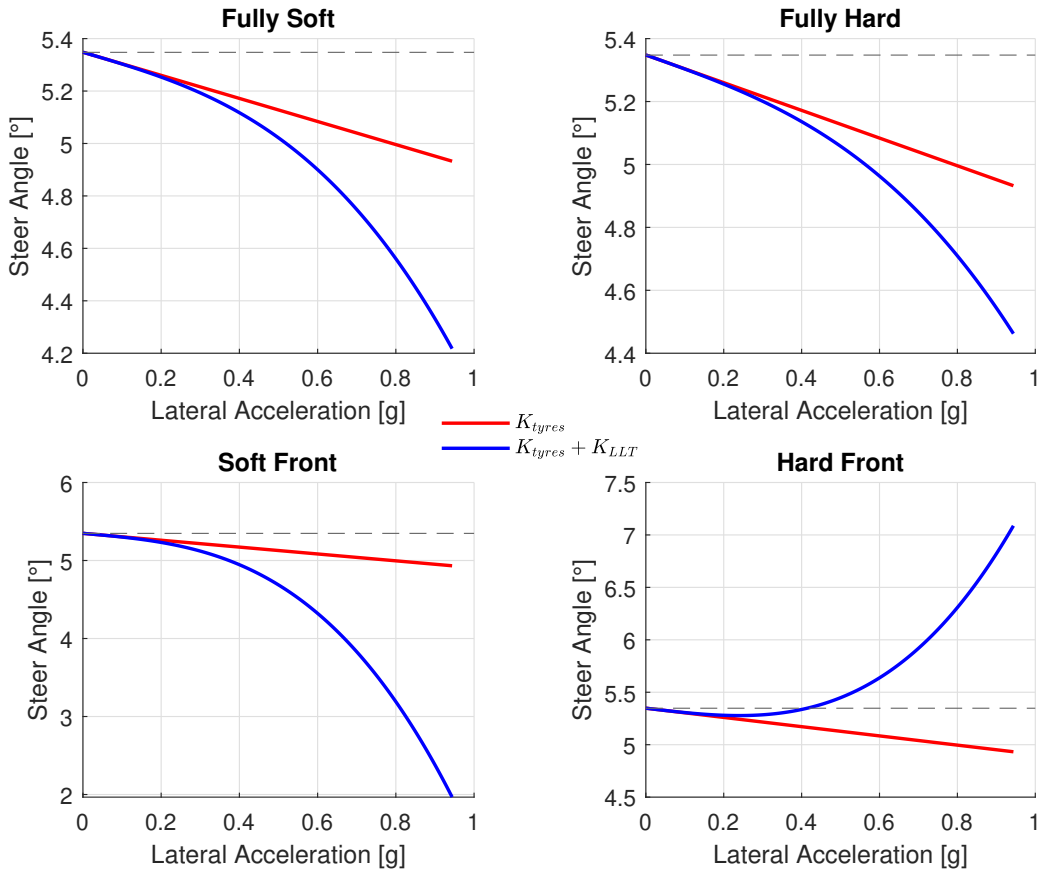

Figure 3.2. First Principle Analytical Steering Angle vs. Lateral Acceleration

Figure 3.3 presents an insightful perspective indicating that manipulating the roll stiffness at a specific axle through the springs can result in more substantial load transfer on that particular axle. This revelation holds significance as it offers crucial insights into influencing the steering attributes of the vehicle concerning understeer or oversteer tendencies. Leveraging this foundational understanding alongside first principle analysis, the next phase involves conducting comprehensive simulations using the nonlinear model of the vehicle and suspension system. This approach is aimed at delving deeper into the effects of these manipulations and their impact on the vehicle's dynamic behaviour and steering characteristics.

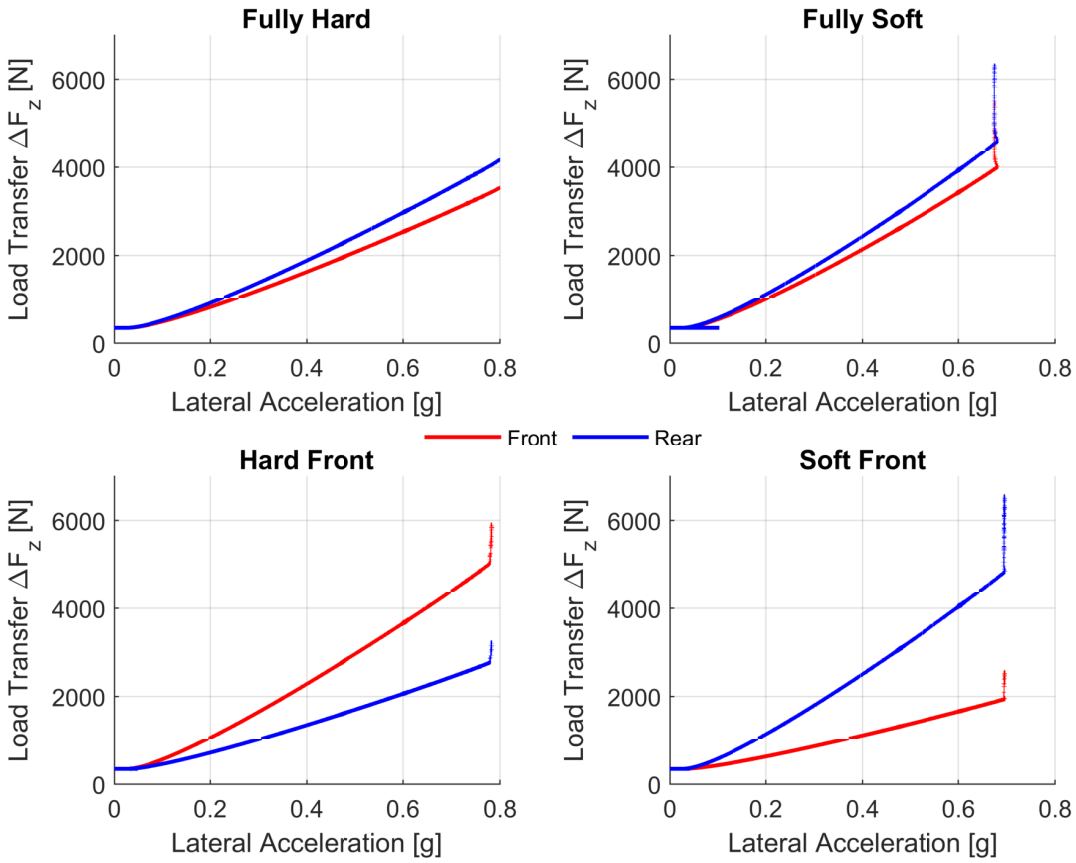

Figure 3.3. First Principle Analytical Load Transfer

3.3 Constant Radius Test

To investigate the effect of the suspension characteristics on the vehicle's handling characteristics related to a change in the understeer/oversteer effects, a constant radius test was performed where the speed was increased linearly from 0 km/h to a desired speed of 60 km/h, however, the model stops accelerating when one of the wheels experiences a low vertical force due to wheel liftoff and the model calculates the drive force required to move the vehicle. A comparison is done to find the maximum between the drive force divided by four and the minimum vertical force of the tyres. The maximum force is then multiplied by the diameter of the wheel to output the desired torque. The minimum radius for the constant radius test is recommended to be 30 metres; therefore, 30 metres will be used as the radius for the simulation. The turn is performed as a counter-clockwise (left) turn. The suspension system simulated is a model of the $4S_4$CVD suspension system mentioned in Section 2.4, where the spring and damper characteristics can be set to *hard* and *soft*. These characteristics are related to the gas volume and the damper scaling factor of the hydropneumatic springs of the $4S_4$CVD. The model also allows for ride height change by extending and retracting the struts of the suspension, which will also be investigated. A driver model developed by Kapania & Gerdes (2015) is used to manoeuvre the vehicle through the test and maintain the position of the vehicle as it follows the desired path provided in MATLAB. Table 3.1 indicates the configurations for the various suspension configurations that are investigated:

Table 3.1. Suspension Configurations for Constant Radius Test Simulation

Suspension Configuration	Spring Characteristic	Damping Characteristic
Fully Hard	Stiff on all corners	Highest damping on all corners
Fully Soft	Soft on all corners	Lowest damping on all corners
Hard Front	Stiff on front struts, soft on rear struts	Highest damping on front struts, lowest on rear struts
Soft Front	Soft on front struts, stiff on rear struts	Lowest damping on front struts, highest on rear struts
Hard Inside	Stiff on inside struts, soft on outside struts	Highest damping on inside struts, lowest on outside struts
Soft Inside	Soft on inside struts, stiff on outside struts	Lowest damping on inside struts, highest on outside struts

3.3.1 Constant Radius Test with Altering Suspension Characteristics

Figure 3.4 indicates the steering angle vs. lateral acceleration for the simulation data and the first order analytical data. The vehicle adheres to the Ackermann angle of 5.34° at the beginning of the manoeuvre and displays oversteer behaviour for all suspension configurations for the simulation data. This is expected as the weight balance of the vehicle is slightly rear-biased. It is apparent that the stiffer configurations maintain neutral steer throughout the manoeuvre and go into limit understeer at higher lateral accelerations, showing the effect of the cornering stiffness on the tyres. As the load transfer increases, the ability to manoeuvre around the turn begins to drop as the tyres become saturated and reach their limit. The vehicle can also maintain a neutral steer characteristic up to 0.4g. Therefore, it is possible to maintain a neutral steer characteristic within reasonable safety bounds regarding lateral acceleration, allowing the driver to maintain a turn and receive feedback from the vehicle after reaching a certain point. There may be a case to use the hard front suspension configuration to maintain the most neutral-steer characteristic; however, the understeer gradient towards higher lateral accelerations is steeper than the fully hard configuration, which could lead to a sudden loss of control.

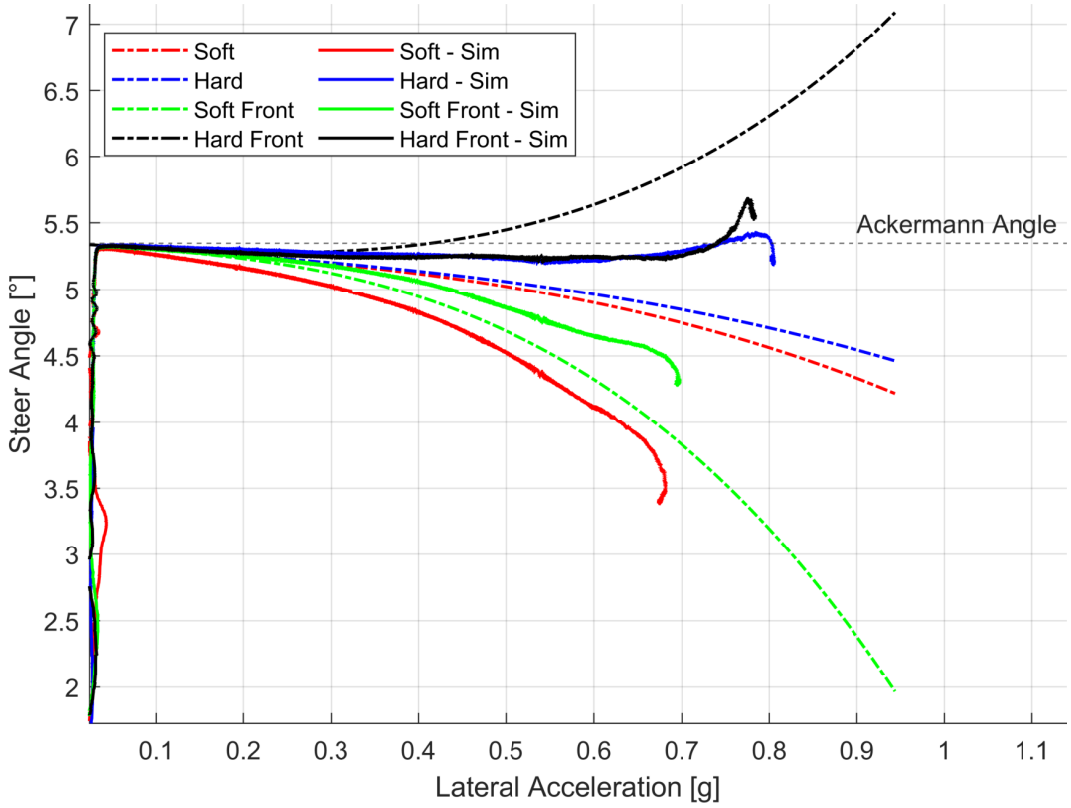

Figure 3.4. Steering Angle vs Lateral Acceleration for CRT

In the analytical calculations, the fully hard suspension exhibits oversteer throughout the manoeuvre. In the simulation, it initially oversteers slightly, then transitions to limit understeer, possibly due to the suspension system's nonlinearity compared to the analytical model. The simulation data trends align with the analytical data, confirming the phenomena, although differing in steer angle magnitude. The soft front configuration consistently generates oversteer from the outset of the manoeuvre, with increased lateral acceleration causing greater load transfer to the rear tyres than the front ones. Comparing the fully hard configuration, both the simulation and analytical models agree in trend until lateral acceleration reaches 0.3g. Subsequently, the simulation data indicates a neutral steer before transitioning to understeer, whereas the analytical model predicts constant understeer throughout the manoeuvre. This discrepancy arises from the extremely stiff nature of the non-linear hard suspension in the analytical model, resulting in minimal spring displacement and reduced differences in vertical force between the inside and outside tyres, thereby decreasing lateral load transfer and promoting a more neutral steering response. The analytical model's assumption of linear deflection in changing roll stiffness doesn't accommodate the suspension's nonlinearity, leading to a consistently oversteering vehicle in the analytical model.

The largest difference in trend is the hard front configuration. The simulation data indicates that the hard front configuration leads to the vehicle experiencing neutral steer throughout the manoeuvre until it reaches limit understeer while the analytical data indicates that the vehicle constantly understeers. The difference is attributed to the complexity and non-linearity of the suspension system in the simulation model as the load transfer is equal for the front and rear for the simulation data while the analytical model experiences larger load transfer at the front and the rear, leading to the understeer characteristic shown. This difference can also be characterised by the effect of roll steer that is present in the simulation model due to the complexity of the suspension geometry and kinematics.

Figure 3.5 presents a comprehensive visualisation of the load transfer dynamics throughout the entire manoeuvre. This visualisation confirms the alignment of trends between substantial load transfer on a specific axle and the corresponding steering behaviour it induces. In the case of the soft front configuration, a more pronounced load transfer towards the rear leads to an increased roll moment on the rear axle, consequently resulting in an oversteer tendency. Conversely, the hard front configuration shows noticeable disparities in the simulation results, showcasing a relatively balanced load transfer until reaching the maximum speed. These findings indicate varying load distribution patterns based on the suspension configuration, influencing the vehicle's steering characteristics differently.

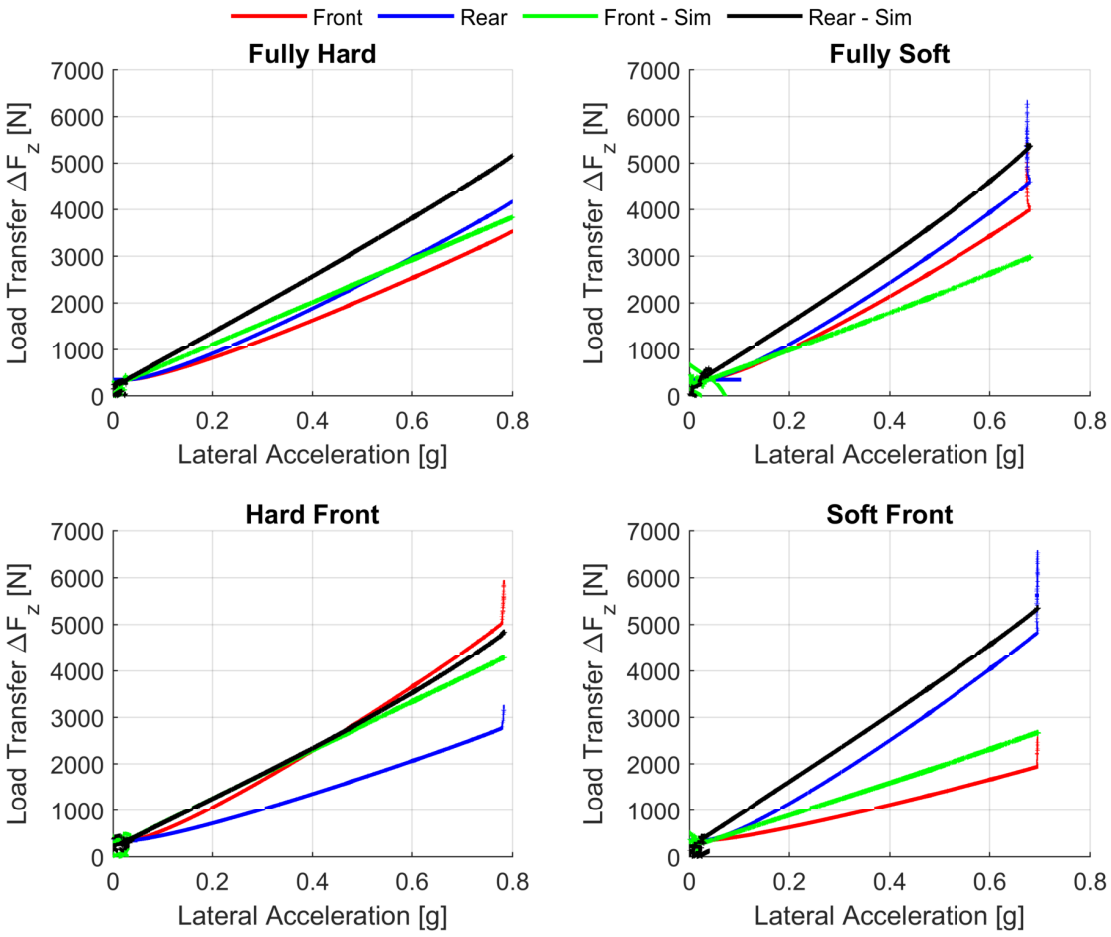

Figure 3.5. Analytical & Simulation Load Transfer through CRT

Figure 3.6 visualises the steer angle against the lateral acceleration of the vehicle for the CRT, indicating the different suspension configurations investigated. It is evident that the hard inside suspension configuration also can maintain a neutral steer characteristic with slight understeer when the lateral acceleration increases. The soft inside leads to an oversteer characteristic, similar to the fully soft suspension configuration. This is attributed to the suspension configuration being stiff on the outside and therefore, the suspension struts will not deflect significantly. This leads to larger lateral load transfer being experienced when compared to suspension configurations that have all struts set to the same stiffness and damping. Additionally, due to the rear bias of the weight balance of the vehicle, the rear outside tyre experiences more load than the front outside tyre, leading to disproportionate lateral load transfer where the rear experiences larger load transfer compared to the front. This leads to oversteer.

The results indicate that the hard inside can be used as an additional suspension configuration which improves the handling of the vehicle due to its neutral steer characteristic, reducing the risk of accidents occurring to a loss of control due to oversteer or a collision due to understeer. This configuration influences the lateral load transfer in a non-intuitive manner as intuition would indicate that having a stiffer outside would lead to better handling and, shown later, less roll but this is not the case.

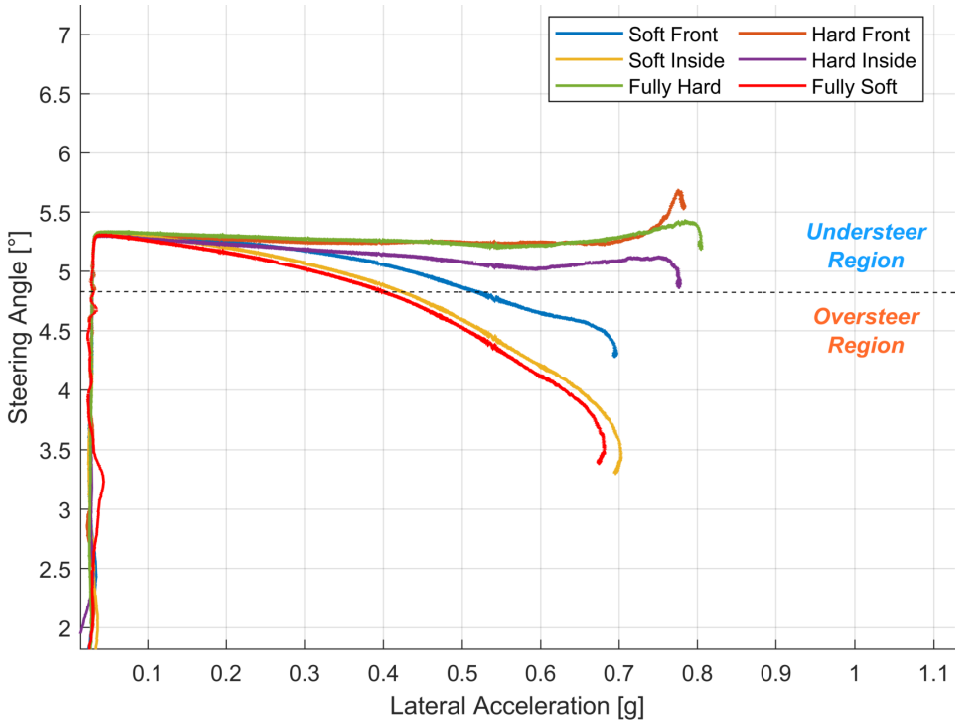

Figure 3.6. Steering Angle vs Lateral Acceleration for CRT - Suspension Configurations

Figure 3.7 indicates the roll angle versus the lateral acceleration through the manoeuvre. This highlights the roll reduction of each configuration when compared to the soft suspension. As expected, the stiff suspension configurations can alleviate the vehicle roll through the turn, as the suspension will not be as compliant and compress as easily as the soft suspension configuration. Figure 3.5 illustrates that there are some intuition-altering results. The hard inside suspension configuration leads to the vehicle experiencing less roll than the hard outside suspension configuration, which goes against intuition as a stiffer outside would seem to alleviate roll to a more significant extent. However, this phenomenon is due to the nonlinearity of the suspension spring and damper characteristics. The vehicle's heading was in an anti-clockwise direction, and therefore, the vehicle would be experiencing roll towards the right. Having a hard outside configuration leads to the suspension exerting a higher force due to the displacement it is experiencing, leading to the outside of the vehicle being a pivot point, and this leads to an increase in CG height. This leads to the vehicle rolling more. When the configuration is the hard inside configuration, the outside suspension will exert a lower force for the same displacement experienced by the hard outside configuration, leading to less roll. This phenomenon of "jacking" was highlighted in Section 2.2.5.2 and is displayed during the manoeuvre.

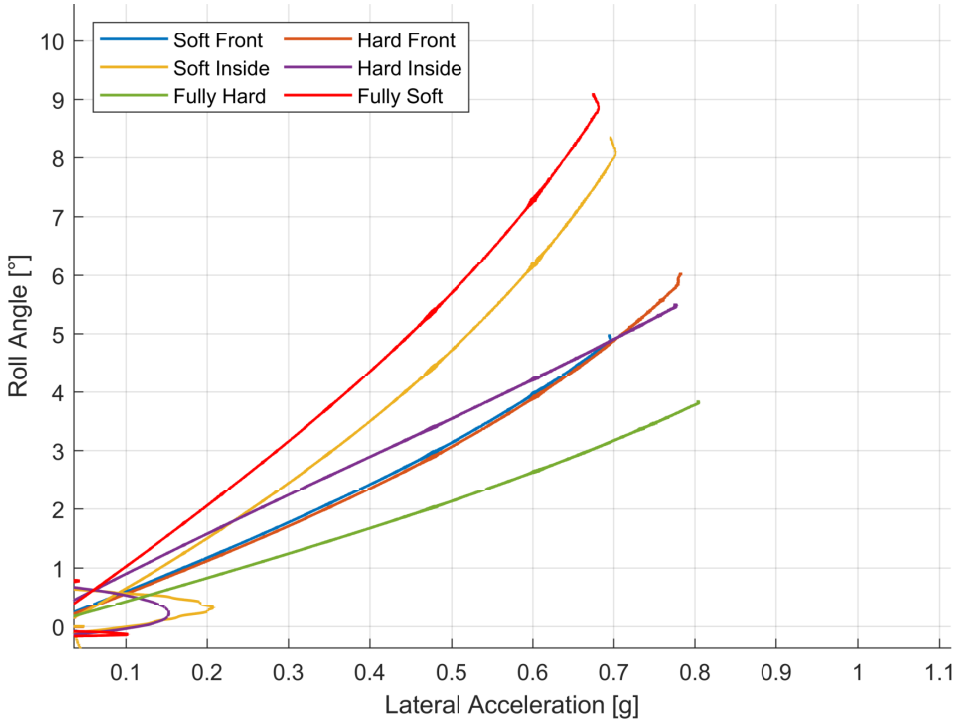

Figure 3.7. Roll Angle vs Lateral Acceleration through CRT

Figure 3.8 further illustrates the jacking effect. The CG height of the vehicle when in the soft inside suspension configuration increases at a higher rate than all other configurations. This increase in CG height results in more roll. Independent suspensions are susceptible to jacking forces whereas solid/beam axle suspensions generally do not exhibit jacking. (Gerrard (1999)) Therefore, this analysis can be applied to various independent suspensions; it is not exclusive to the $4S_4$CVD system used in the simulation. The jacking forces experienced in this simulation are mostly due to factors such as suspension spring and damping characteristics as the research looks into asymmetric configurations of spring rate and damping. As the vehicle experiences various load transfer situations attributed to the different configurations, The distribution of lateral forces can create vertical lift or jacking forces, particularly if the suspension geometry promotes such effects. The damping of the suspension does not play a large role in the effect as damping is related to controlling the rate at which the suspension compresses or rebounds when subjected to external forces, such as bumps or vibrations or when performing dynamic manoeuvres and the CRT does not excite the suspension in this manner. Therefore, it can be said that the damping won't have a large effect on mitigating the jacking effect. While damping doesn't directly cause suspension jacking, inadequate or mismatched damping characteristics could exacerbate the effects of jacking. Improper damping settings may lead to situations where the suspension can't adequately absorb or respond to sudden wheel movements or impacts. This insufficient response might contribute to a suspension's tendency to stiffen or lock under specific conditions, potentially aggravating the occurrence of jacking.

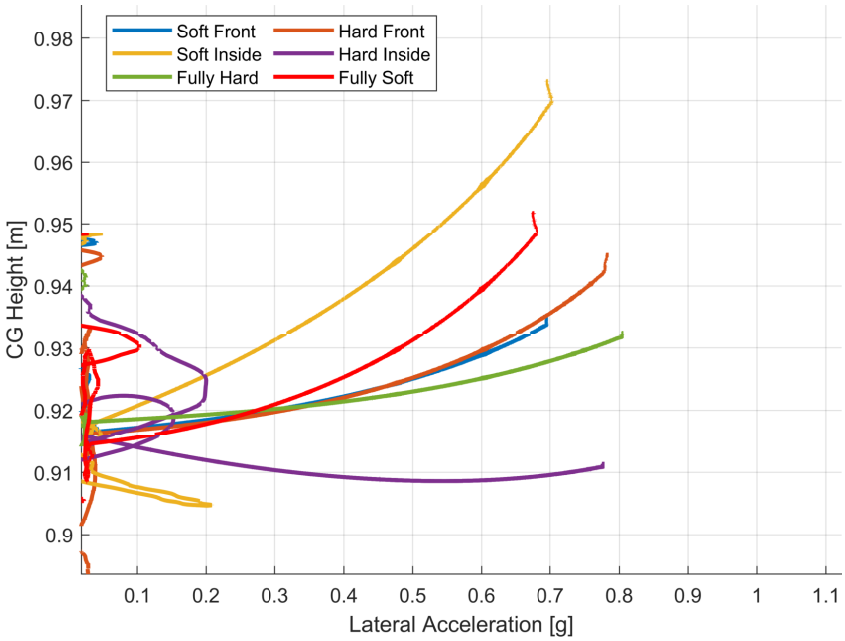

Figure 3.8. CG Height vs Lateral Acceleration through CRT

The key findings of the analysis are summarised below:

- During vehicle manoeuvres, the suspension characteristics play a pivotal role in determining the CG height. This influence primarily stems from the jacking forces exerted on the suspension system. These forces, arising from the interplay between the vehicle's dynamics and the suspension's response to external inputs like sudden changes in road surfaces or aggressive steering actions, significantly impact how the vehicle behaves. When the suspension experiences these jacking forces, it affects the vehicle's overall vertical movement, causing alterations in the CG height.
- Efficient management and meticulous adjustments of the suspension components, including damping systems, spring rates, and the overall structural design, offer a robust avenue for mitigating the impact of jacking forces on the suspension. This strategic approach not only helps in alleviating the potential effects of these forces but also serves to dynamically influence the CG height during various manoeuvres. Moreover, the integration of ride height control into the suspension system represents another pivotal method to counter jacking forces. By optimising ride height, the system can effectively manage the impact of these forces, contributing to a notable enhancement in the vehicle's handling capabilities, overall stability, and its overall performance. This proactive measure provides a means to fine-tune the vehicle's response to varying external stimuli, offering more precise control and a heightened level of dynamic adaptability.

3.3.2 Constant Radius Test with Ride Height Change

Simulations were performed to show how the vehicle dynamics are affected by a lowering/raising of the front and rear struts of the suspension to investigate the effect of altering the ride height on the vehicle. The front suspension struts have allowable travel of 250 mm, while the rear suspension struts have allowable travel of 300 mm. In the following analysis, the suspension displacements were altered statically before the vehicle started the constant radius manoeuvre and displaced to the maximum allowable travel. There is an assumption that the tyre deflection does not factor into the location of the roll centre height. The analysis will look at two aspects of using the ride height control, namely anti-roll implementation and using the control to affect the steering characteristic of the vehicle. This investigation will explore the effects of raising the front and rear of a vehicle to highlight how altering the roll axis inclination impacts the vehicle's dynamics. Without extensive analysis, it is evident that increasing the roll centre height at one axle decreases the lateral load transfer at the opposite axle, assuming all other factors remain constant. This phenomenon occurs because elevating the roll centre height at a given axle brings the roll axis closer to the vehicle's centre of gravity (CG), thereby reducing the roll angle component. Since the roll centre height of the opposite axle remains unchanged, the direct lateral force component does not increase. Consequently, the overall effect is a reduction in lateral load transfer on the axle opposite to the one with the raised roll centre height. This effect can be strategically used to induce more understeer or oversteer by adjusting the vehicle's height at specific axles.

Figure 3.9 delineates the relationship between the steering angle and lateral acceleration throughout the manoeuvre, with specific emphasis on the variations in height for the fully hard suspension configuration. It is evident that lowering the vehicle induces a more pronounced understeer characteristic compared to the baseline configuration. Conversely, elevating the vehicle at either end engenders a more significant oversteer characteristic relative to the baseline. The most substantial deviation is observed in the rear lift scenario, where the vehicle exhibits oversteer behaviour from the onset and fails to achieve a neutral steer characteristic at any point during the manoeuvre. In contrast, lowering the rear results in a neutral steer characteristic up to a lateral acceleration of 0.6 g, beyond which the vehicle gradually transitions into understeer. Notably, this configuration also attains the highest lateral acceleration. The data clearly illustrates the pivotal role of the rear suspension in influencing the vehicle's steering characteristics. Adjusting the ride height at the rear axle has a profound impact on the vehicle's handling dynamics. The rear-biased weight balance of the vehicle means that alterations at the rear have a greater influence than those at the front. This is because the rear lift configuration results in a significant shift towards oversteer, indicating a substantial increase in the lateral load transfer to the rear tyres, thereby diminishing the grip available at the rear and leading to oversteer. On the other hand, lowering the rear mitigates this effect, maintaining a balanced neutral steer up to higher lateral accelerations before transitioning to understeer.

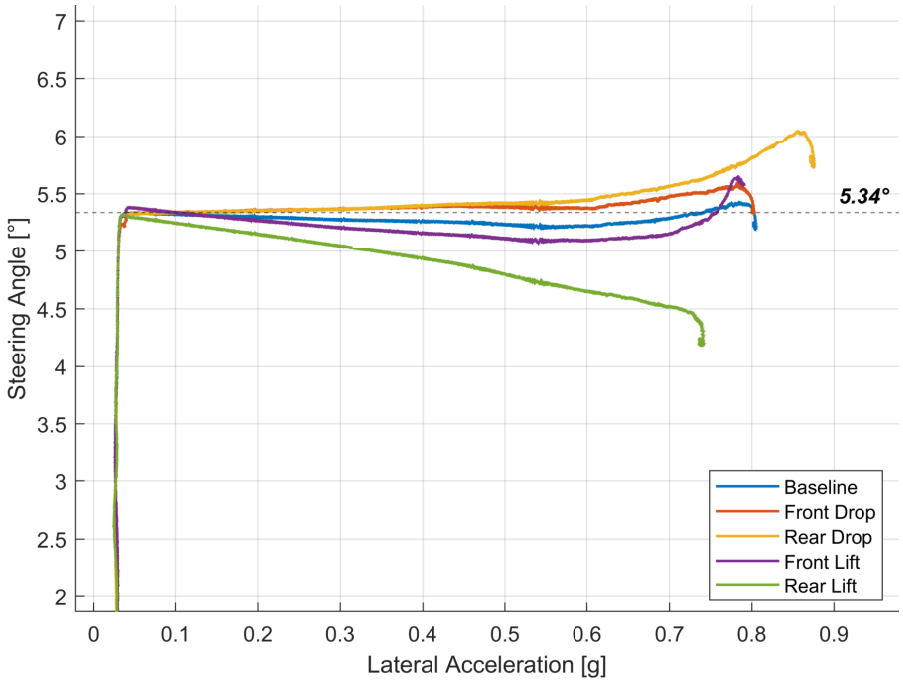

Figure 3.9. Steering Angle vs Lateral Acceleration for CRT with Ride Height Change - Hard Configuration

Figure 3.10 provides a comprehensive overview of the dynamic behaviours observed during the CRT manoeuvre, specifically focusing on the roll angle and the lateral load transfer ratio (LTR). An insightful analysis of these parameters unveils a noteworthy trend that advocates for the lowering of the rear as an optimal course of action for both enhancing handling characteristics and mitigating the risk of rollover incidents. Remarkably, the act of lowering the rear exhibits a substantial impact, notably yielding the most favourable outcomes in terms of minimising the roll angle, along with a gradual increment in the lateral load transfer ratio. Intriguingly, despite experiencing significantly increased lateral acceleration, this configuration results in the most controlled and manageable dynamics. Conversely, it becomes evident that alterations in the front axle, whether lifted or lowered, do not significantly influence the vehicle's dynamics. The roll angle and LTR values for these adjustments closely resemble those of the vehicle's baseline configuration, suggesting a limited impact of front-axle modifications on the overall behaviour during the CRT manoeuvre.

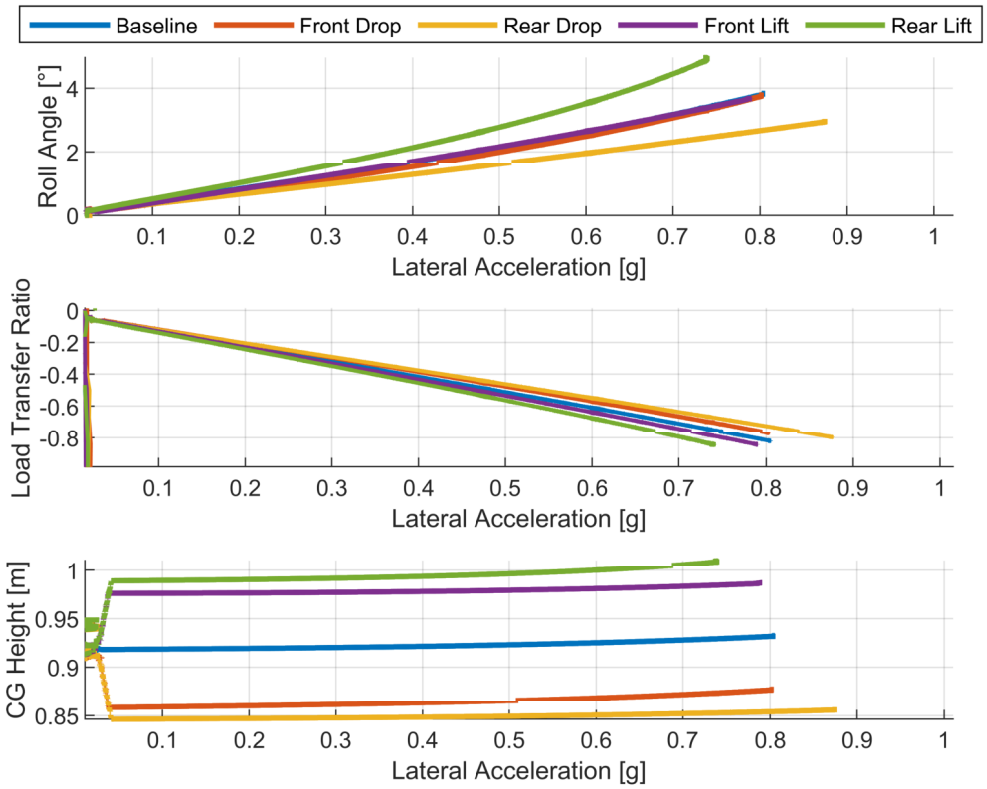

Figure 3.10. Roll Angle, Load Transfer Ratio, & CG Height vs Lateral Acceleration for CRT with Ride Height Change - Hard Configuration

The data from the simulations indicates that:

- Manipulating the roll stiffness of an axle significantly impacts the steering behaviour and handling dynamics of the vehicle. Both the initial order analysis and the comprehensive simulation data consistently demonstrate alignment in the trend and magnitude of these alterations. This signifies the validity and credibility of modifying suspension characteristics to actively influence the distribution of load transfer within the vehicle's dynamics. The correlation between the analytical and simulated results validates the effectiveness of adjusting suspension properties to deliberately modulate the vehicle's response to lateral forces, showcasing its potential to finely tune handling characteristics and enhance overall driving performance.
- Implementing ride height control offers a viable avenue to actively influence and modulate the steering behaviour of a vehicle. This control mechanism presents an opportunity to induce specific handling characteristics such as understeer or oversteer by strategically adjusting the vehicle's ride height. Elevating the front or lowering the rear height configuration tends to encourage understeer tendencies, effectively influencing the vehicle's handling dynamics by promoting a propensity for a more stable, straight-line trajectory through corners. Conversely, dropping the front or elevating the rear height configuration tends to promote oversteer characteristics, which lead to a more agile and responsive turning behaviour, favouring a sharper and more dynamic handling response when navigating corners or curves.

A control system was developed in the MATLAB/Simulink environment, where the error between the front left and rear left slip angle was used to measure whether the vehicle was understeering or oversteering to implement these conclusions. With that error, it was used in a PID controller, which attempts to lift or drop the axle, leading to a neutral steering characteristic for the vehicle. For this simulation, understeer is classified as when the front slip angle is larger than the rear slip angle, and oversteer is classified as when the rear slip angle is larger than the front slip angle. Figure 3.12 illustrates the control flowchart.

The use of various suspension configurations was not investigated for this analysis as it would be beneficial to attempt to use the soft suspension and get it to perform on par with the stiff suspension. This will allow for excellent ride comfort while having the handling characteristics of the stiff suspension. Figure 3.11 illustrates the slip angle error throughout the constant radius test and the output displacement of the PID. It is apparent that the vehicle was slightly oversteering at a constant change in the slip angle difference, and therefore, the PID had an output of lifting the front to combat the oversteer.

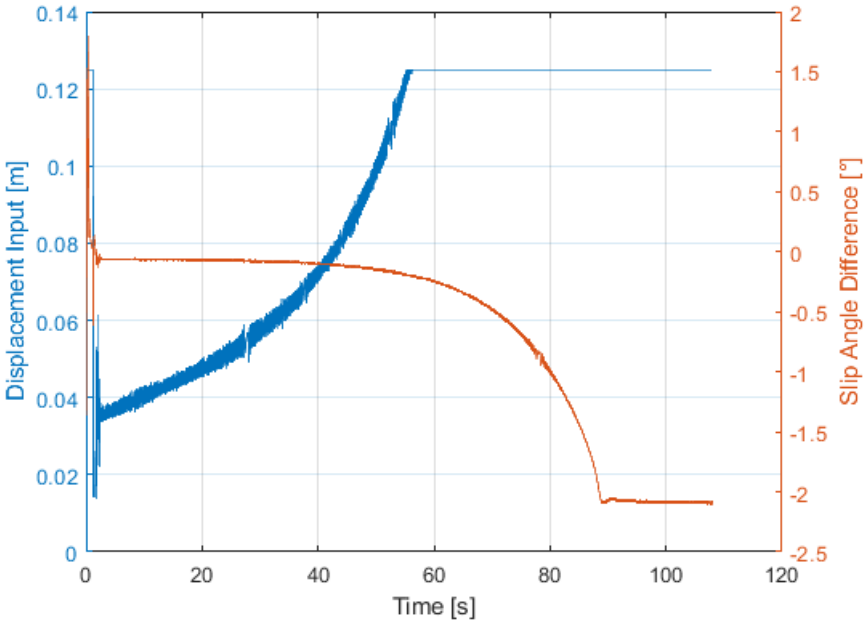

Figure 3.11. PID Displacement Input & Slip Angle Error

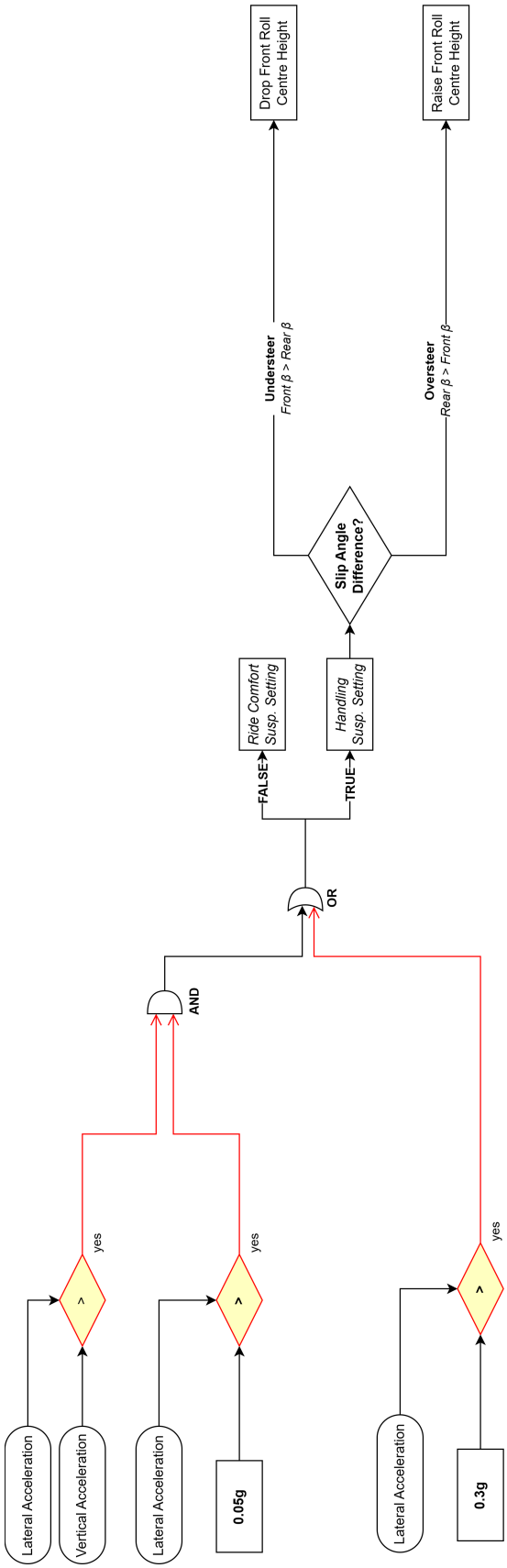

Figure 3.12. Understeer Control Logic Flow Chart

Figure 3.13 presents an insightful analysis demonstrating the functionality of the PID system in achieving and maintaining a neutral steer characteristic within passenger car driving scenarios, up to lateral acceleration levels of 0.4 g. This capability marks a significant advantage as it ensures intervention within safe operational limits, aiding in the management of potentially hazardous speeds and high-speed driving dynamics. However, it is important to note a critical point in the system's behaviour: when the PID system reaches the limit of the strut's displacement, the vehicle swiftly transitions into an oversteer state, differing markedly from the behaviour observed in the baseline soft suspension configuration. This sudden shift towards oversteer could potentially raise safety concerns, given the vehicle's instability without prior driver input or feedback into the system, thereby highlighting a potential risk factor.

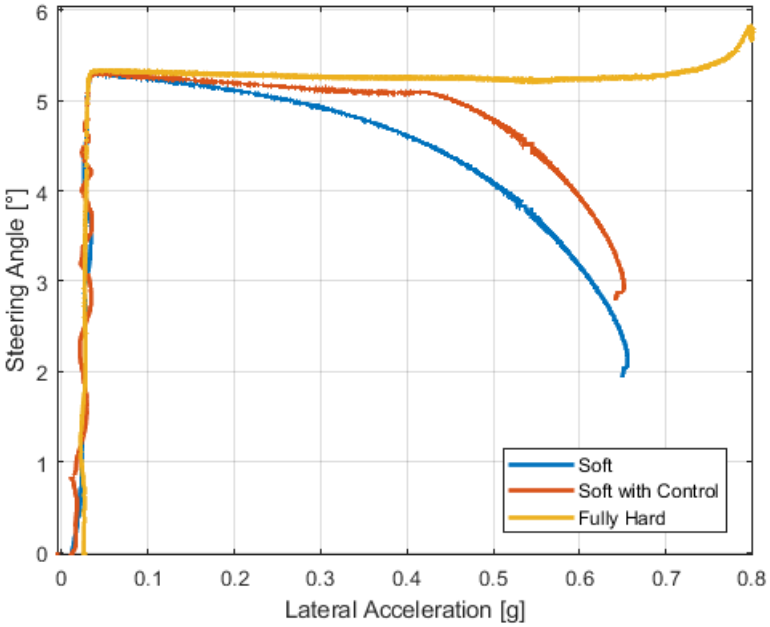

Figure 3.13. Steering Angle vs. Lateral Acceleration for Understeer Control for CRT

3.3.3 Constant Radius Test with Anti-Roll Control

In the process of refining the controller's capabilities, the development of the ride height control extended to encompass anti-roll control, aiming to effectively curtail the vehicle's roll tendencies during manoeuvres. This comprehensive control system incorporates specific triggers to activate handling modes, with lateral acceleration serving as a pivotal threshold; if it surpasses 0.3 g, the suspension system transitions into handling mode. Moreover, the system employs the vehicle's roll angle as another significant trigger; when the roll angle exceeds 2.5°, a proportional oil dump occurs within the inside struts, strategically directed to counteract and limit the vehicle's roll tendency. This integrated approach aims to deliver heightened control over the vehicle's roll dynamics during manoeuvring, emphasising an adaptive response based on lateral acceleration and roll angles to enhance overall handling and stability. Figure 3.14 illustrated the logic that the anti-roll control follows:

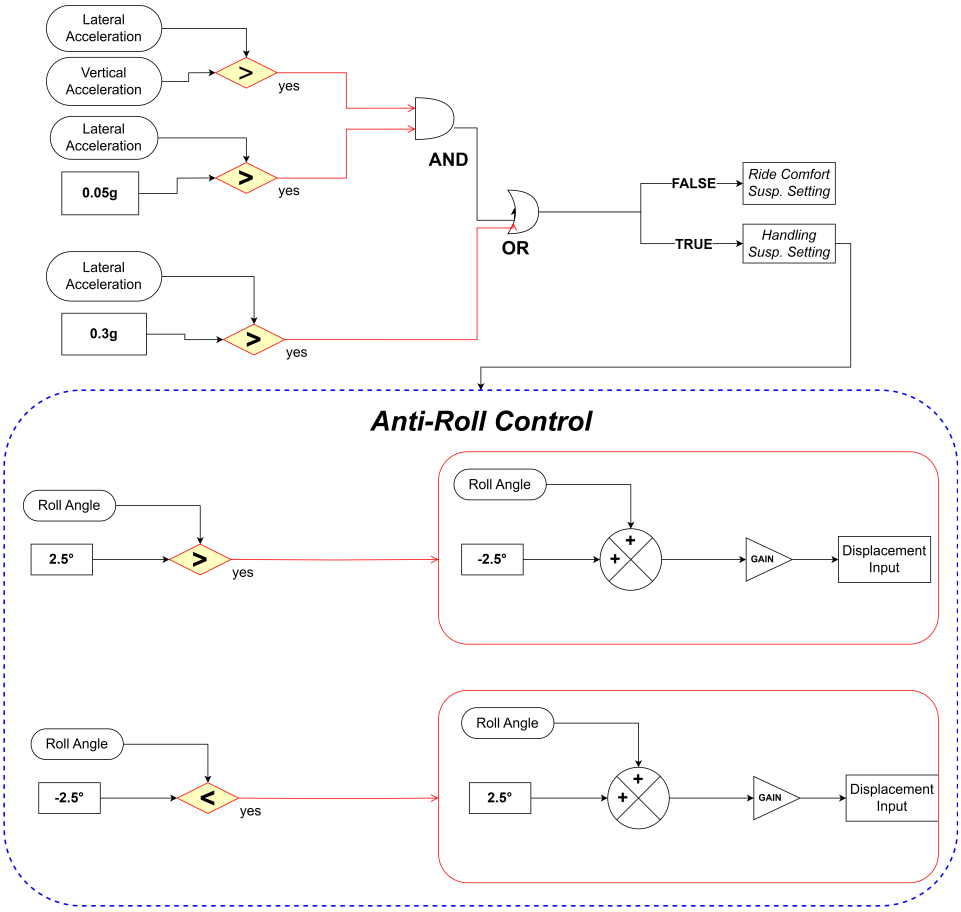

Figure 3.14. Anti-Roll Control Flowchart

Upon considering options to limit the vehicle's roll, the feasibility of extending the outside struts was deliberated, yet it was deemed impractical due to the potential consequences. Such an alteration would not only restrict the vehicle's roll but also inadvertently elevate the CG height, consequently amplifying the jacking effect and augmenting the vehicle's predisposition to rollover. Figure 3.15 provides a visual representation showcasing the roll angle throughout the manoeuvre. Comparing the effects of anti-roll control with the soft suspension configuration reveals that the anti-roll control successfully limits the roll, closely tracking the baseline soft configuration until the lateral acceleration surpasses the predetermined threshold. The anti-roll control engages when the lateral acceleration exceeds the prescribed criteria, which necessitates that it surpasses both the longitudinal acceleration and 0.3 g of lateral acceleration. Eventually, the final roll angle attained by the anti-roll control closely approximates the roll angle exhibited by the baseline stiff suspension. There is a potential for an earlier transition from soft to hard suspension that could potentially reduce the final roll angle further. However, this adjustment might bring the vehicle's behaviour closer to that of the baseline stiff suspension without any control intervention, potentially rendering the anti-roll control superfluous. This relates to the compromise between ride comfort and handling as using the fully hard configuration will result in poor ride with the advantage of being safer than the fully soft configuration. With the semi-active suspension configuration, the compromise is not needed as different discrete or continuously variable settings for the springs and/or dampers are available. The choice can be made to switch the suspension configuration to handling mode when a handling or performance manoeuvre is detected while keeping the suspension in ride comfort mode for the rest of the journey. (Els (2006))

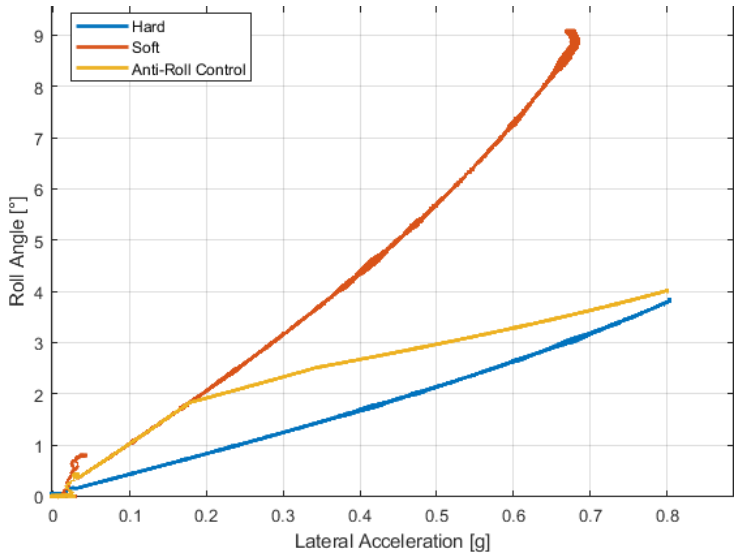

Figure 3.15. Roll Angle vs Lateral Acceleration for Anti-Roll Control for CRT

Figure 3.16 presents the load transfer ratio (LTR) observed throughout the manoeuvre, showcasing distinct behaviours between the anti-roll control and soft suspension configurations. The anti-roll control demonstrates a methodical and gradual increase in LTR, contrasting with the soft suspension configuration which shows a more pronounced initial rise. Despite achieving a lower final LTR value, the soft suspension's rapid elevation in LTR prompts a notable decrease in vertical forces exerted on the tyres, leading to the vehicle not accelerating further. This reduction occurs as the vertical forces on the tyres diminish to levels that stop the model from accelerating the vehicle in order to prevent rollover. It is essential to note the implications of these findings within the context of vehicle dynamics and suspension system design, particularly concerning the trade-offs between LTR dynamics and acceleration performance under varying configurations.

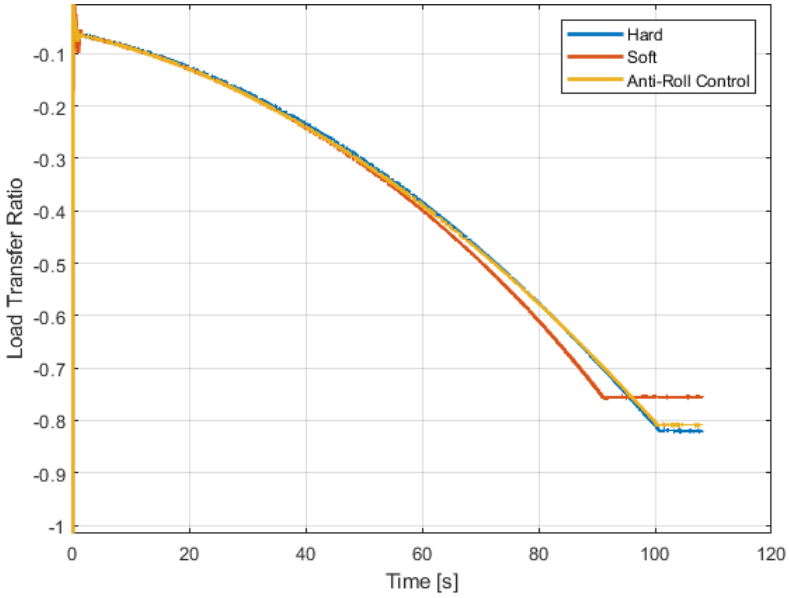

Figure 3.16. Load Transfer Ratio for Anti-Roll Control for CRT

3.4 Double Lane Change

The ISO3888-1 Double Lane Change test (1999) will assess the dynamic handling of the Land Rover. This manoeuvre is designed to evaluate a vehicle's handling and roll sensitivity, covering a wide range of dynamics in a short duration. Initially, the different suspension configurations employed in the Constant Radius Test are explored to understand their impact on handling. Subsequently, anti-roll control is utilised to examine its effect on reducing the vehicle's rollover propensity.

3.4.1 Double Lane Change with altering Suspension Characteristics

The suspension configurations were altered to investigate the effect that the spring and damper configurations may have on the vehicle's dynamic handling. The suspension states follow the same configuration as in the constant radius test, except for the hard inside and soft inside configurations.

Table 3.2. Suspension Settings for Double Lane Change Simulation

Suspension Setting	Spring Characteristic	Damping Characteristic
Fully Hard	Stiff on all corners	Highest damping on all corners
Fully Soft	Soft on all corners	Lowest damping on all corners
Hard Front	Stiff on front struts, soft on rear struts	Highest damping on front struts, lowest on rear struts
Soft Front	Soft on front struts, stiff on rear struts	Lowest damping on front struts, highest on rear struts
Hard Inside	Stiff on inside struts, soft on outside struts	Highest damping on inside struts, lowest on outside struts
Soft Inside	Soft on inside struts, stiff on outside struts	Lowest damping on inside struts, highest on outside struts

For the soft inside configuration, the side of the vehicle on the inside will have low damping and a soft spring characteristic, and this configuration will switch depending on the direction of the vehicle's roll angle. The opposite applies to the hard inside, where the side of the vehicle which is on the inside will have high damping and a stiff spring characteristic. Figure 3.17 illustrates the fully hard suspension setting performs best where it achieves the lowest roll angle throughout the manoeuvre.

The hard front performs second best while the soft front configuration performs close to the fully soft configuration. This behaviour is due to the phenomenon shown in the constant radius test where the hard front configuration experiences more load transfer at the front than the rear and, therefore, experiences understeer. This would lead the vehicle to change lanes with less yaw motion than with the soft front configuration.

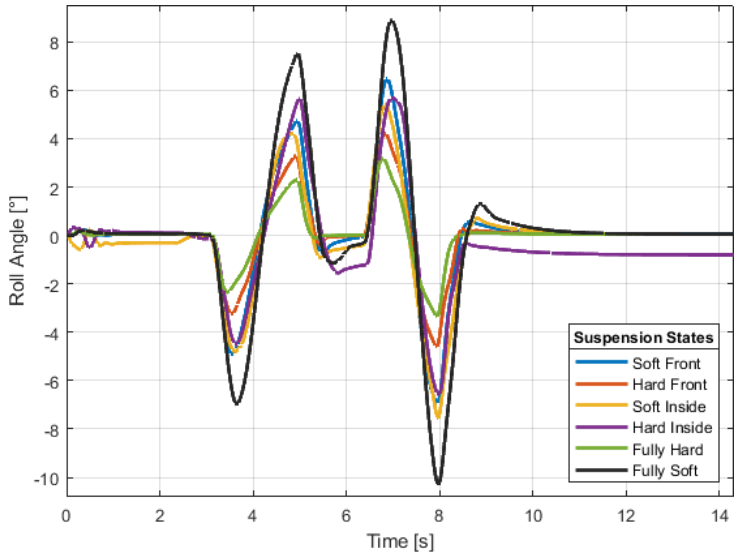

Figure 3.17. Roll Angle for Altering Suspension Settings through DLC

Figure 3.18 illustrates the roll rate of the vehicle through the manoeuvre. The fully hard suspension performs the best, achieving the lowest roll rate during the manoeuvre, and the hard front configuration is second-best. With these results, the usefulness of altering the suspension settings is questioned, as the fully hard configuration will consistently outperform any other configuration investigated. It must be noted that the handling mode would be used as a last resort safety measure to have the vehicle as safe as possible. The hard front configuration, for example, would be used to make the vehicle experience more understeer in daily driving and still perform well enough in emergencies if needed while maintaining better ride comfort. However, the handling mode can be improved with anti-roll control, which will be investigated in the next section.

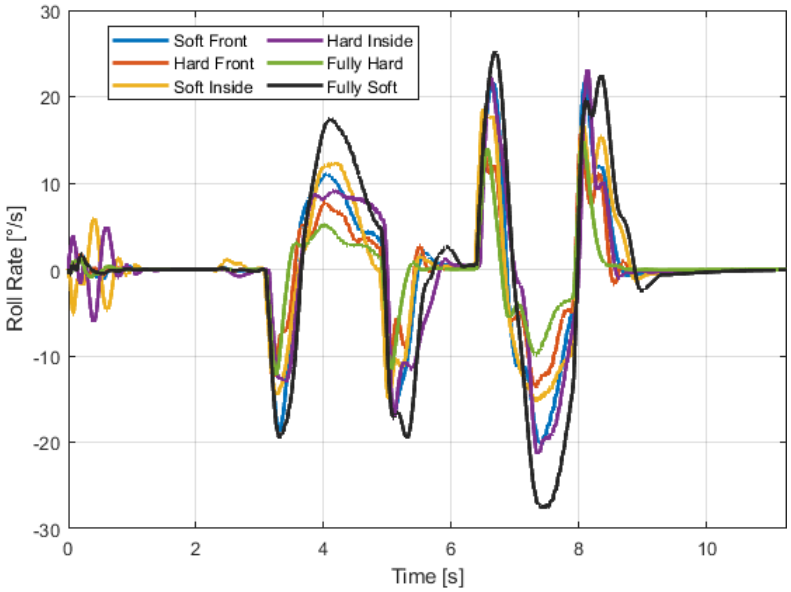

Figure 3.18. Roll Rate for Altering Suspension Settings through DLC

3.4.2 Double Lane Change with Anti-Roll Control

Similar to the constant radius test, the roll control uses the roll angle of the vehicle as a 'trigger' where, if the roll angle is larger than 2.5°, the oil inside the inside struts of the vehicle is dumped to the oil reservoir in proportion to how much the roll angle is in an attempt to limit the roll of the vehicle. Figure 3.19 illustrates the roll angle through the manoeuvre. The anti-roll control decreases the roll angle during the manoeuvre compared to the baseline handling mode configuration. When looking at the most prominent positive peak for the roll angle at 7 seconds, the anti-roll decreases that peak by 14.3% from 3.17° to 2.71°. The improvement is insignificant. However, it is valuable insight as the rollover propensity could be improved upon with changes to the control algorithm. Roll angle for the simulation is measured as the angular displacement of the vehicle body around the x-axis at the CG. Roll angle in the actual vehicle is estimated using a VBox 3i differential GPS (VBOX Automotive (2023)) integrated with the IMU04 (VBOX Automotive (2023)) inertial measurement unit, which captures the vehicle's roll, pitch and yaw rates, the vertical, longitudinal and lateral accelerations and GPS location, vehicle speed and heading. The integrated Kalman Filter in the VBox is used to determine the roll angle.

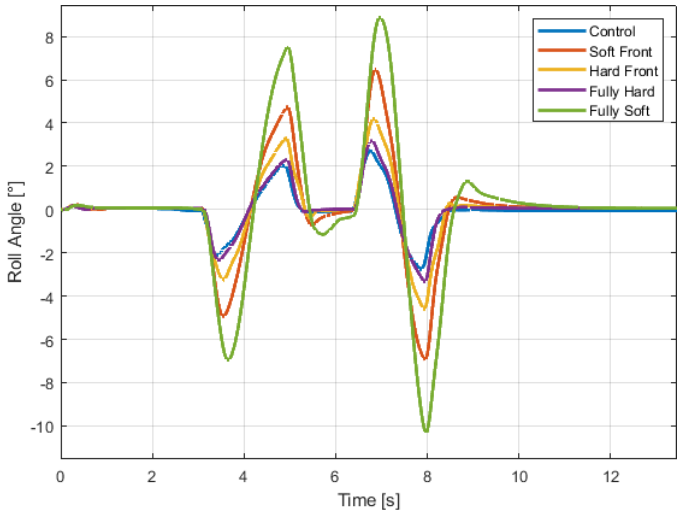

Figure 3.19. Roll Angle for Anti-Roll Control through 60 km/h DLC

The theoretical oil added to and pulled from the struts is shown in Figure 3.20. The amount of oil used was not significant, and the control led to a reduction in roll angle. It is fair to assume that more significant oil flow into and out of the strut will lead to better results, which requires more tuning of the proportional gain of the anti-roll control.

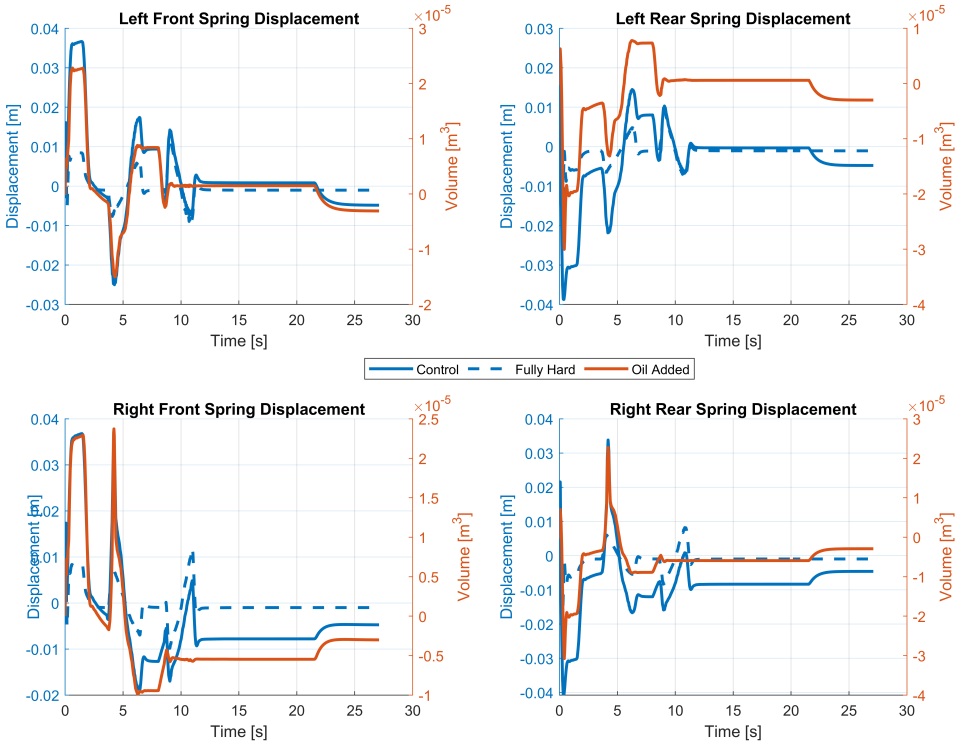

Figure 3.20. Spring Displacement for Anti-Roll Control through 60 km/h DLC

3.5 Fishhook 1B Test

The Fishhook 1B test investigates the lateral dynamics of the vehicle and is an excellent test in order to investigate the rollover propensity. The Slowly Increasing Steer test [Forkenbrock et al. (2003)] must be performed initially to to characterise the lateral dynamics of the specific vehicle being investigated in order to perform the Fishhook 1B Test. For the following Slowly Increasing Steer Test, 270° will be used as the maximum angle and the vehicle speed will be 80 km/h, which is shown in Figure 3.21:

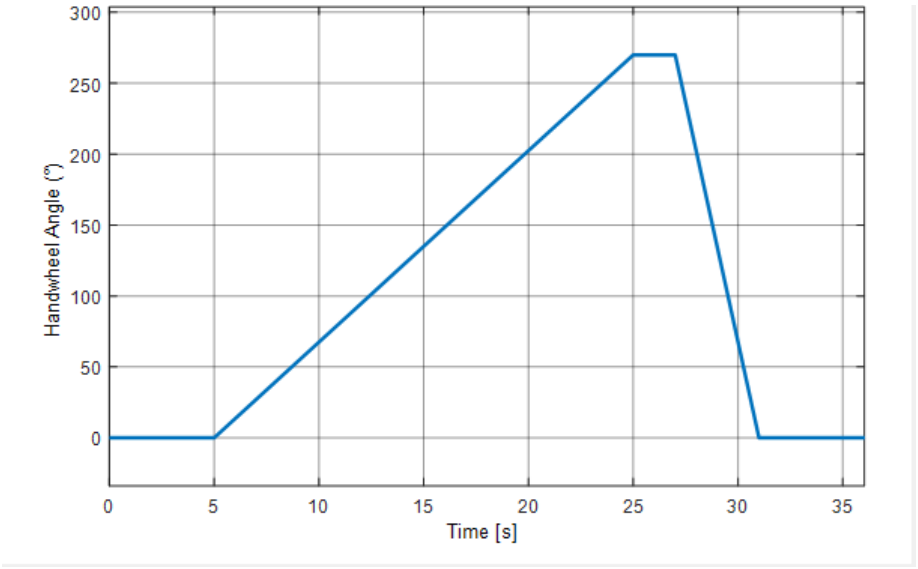

Figure 3.21. Slowly Increasing Steer Steering Wheel Input [Forkenbrock et al. (2003)]

The ADAMS model uses the angle at the tyres to steer as an input and not the handwheel angle. Therefore, the steer angle at the front tyres needs to be calculated. The vehicle's steering ratio to obtain the relevant steer angle. An experiment was conducted with the Land Rover Defender 110 that the simulation model is based on where the steering angle was rotated lock-to-lock, the angles at the wheel were calculated using trigonometric triangles, and the average steering ratio was 21.3.

After this, the input shown in Figure 3.21 was used to find the handwheel angle at which the vehicle experiences 0.3g in lateral acceleration during the Slowly Increasing Steer Test, which was found to be 25.39°, shown in Figure 3.22:

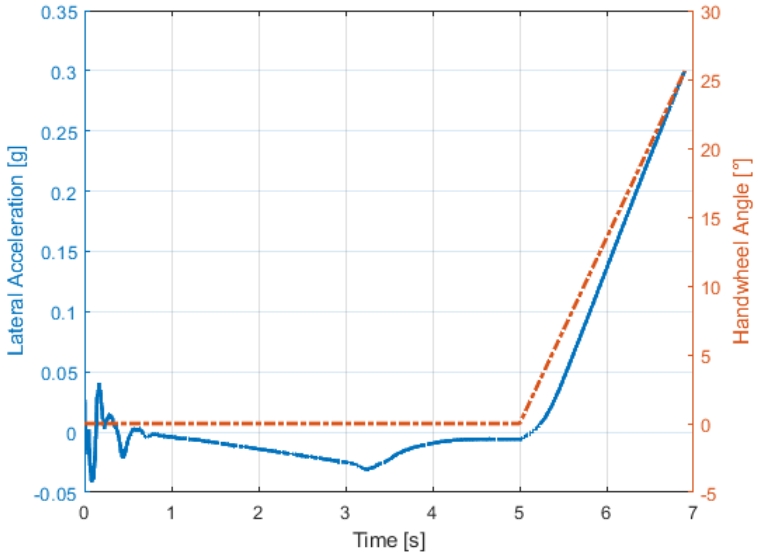

Figure 3.22. Slowly Increasing Steer Handwheel Angle & Lateral Acceleration

After obtaining this angle, it must be multiplied it by a factor of 6.5 in order to obtain the maximum handwheel angle for the Fishhook test, which equates to 165.04°. The angle must be reached with a ramp of 720°/s. The main difference between the Fishhook 1A test and the Fishhook 1B test is that the dwell time after the first ramp in the 1A test is constant regardless of vehicle roll rate and vehicle speed while the dwell time in the 1B test varies. The negative ramp in the handwheel angle begins when the vehicle reaches 1.5°/s in roll rate for the second instance during the manoeuvre. The input is shown in Figure 3.23:

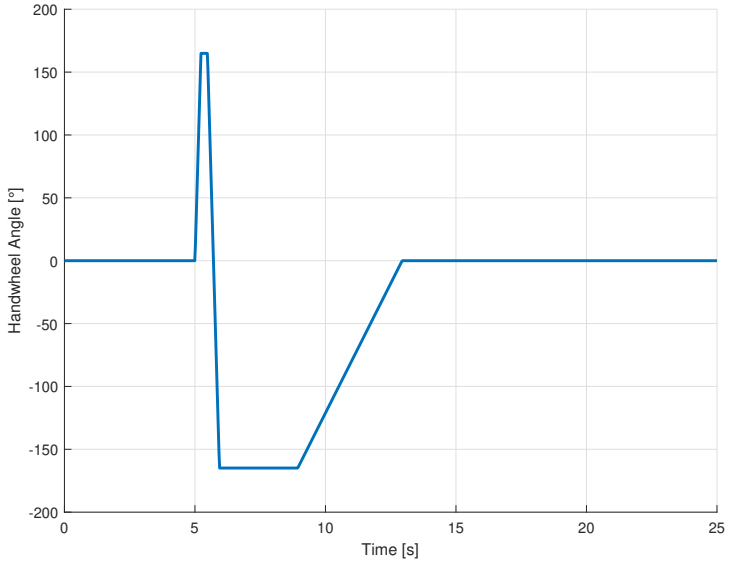

Figure 3.23. Fishhook 1B Test Handwheel Input for Land Rover Defender 110

The vehicle was simulated as driving straight for 5 seconds, reaching a desired entry speed into the manoeuvre, and then the steer angle input would be triggered.

3.5.1 Fishhook 1B Test with altering Suspension Characteristics

The vehicle's yaw rate throughout the manoeuvre is shown in Figure 3.25:

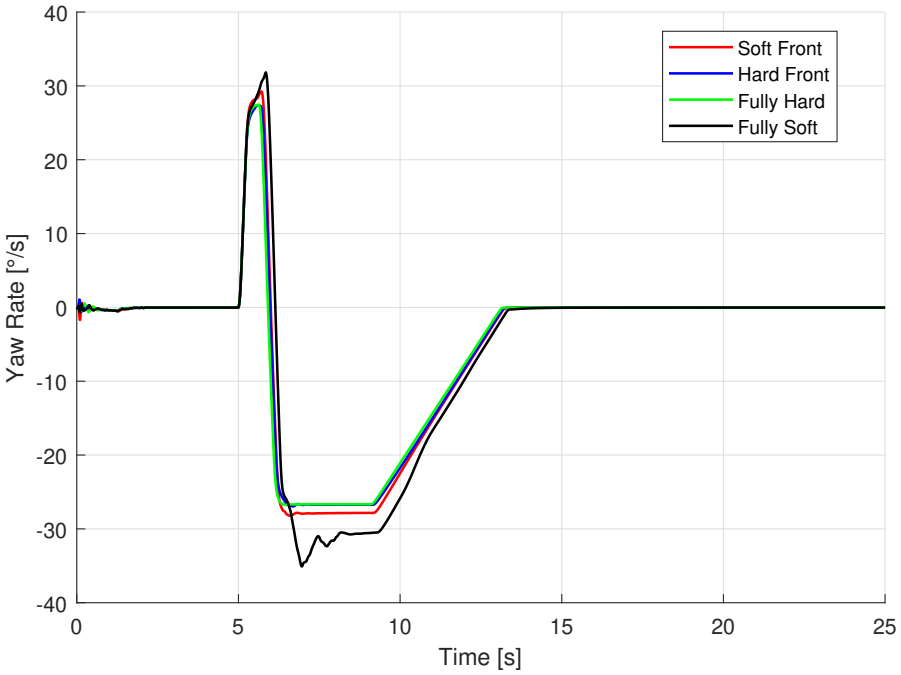

Figure 3.24. Fishhook 1B Test Yaw Rate - 35km/h

The comparison between softer and harder suspension settings reveals distinct characteristics in the vehicle's behaviour during the Fishhook 1B manoeuvre. Specifically, the analysis shows that a soft front suspension configuration results in a higher yaw rate compared to both hard front and fully hard suspension settings. This higher yaw rate with the soft front configuration can be attributed to the increased lateral load transfer at the rear of the vehicle. When the front suspension is softer, the vehicle experiences more body roll, causing greater weight to shift towards the outside rear wheel during a turn. This shift enhances the rear axle's contribution to the vehicle's rotational dynamics, thereby increasing the yaw rate.In contrast, the hard front and fully hard suspension configurations exhibit a noticeably lower yaw rate. These settings reduce the vehicle's body roll, resulting in less lateral load transfer to the rear axle. Consequently, the vehicle's responsiveness to steering inputs is diminished, making it less agile in turns compared to the soft front configuration. Essentially, the hard front and fully hard configurations enhance stability by minimising weight transfer and maintaining a more balanced load distribution between the front and rear axles.Despite their similar performance in terms of yaw rate,

the fully hard configuration might offer additional benefits in terms of overall vehicle stability and handling precision. This setup ensures that the suspension system is optimised for minimal body roll, which can improve the vehicle's contact with the road surface and enhance traction during high-speed manoeuvres. Figure 3.25 indicates the vertical forces on the tyres during the Fishhook 1B manoeuvre for each of the investigated suspension configurations:

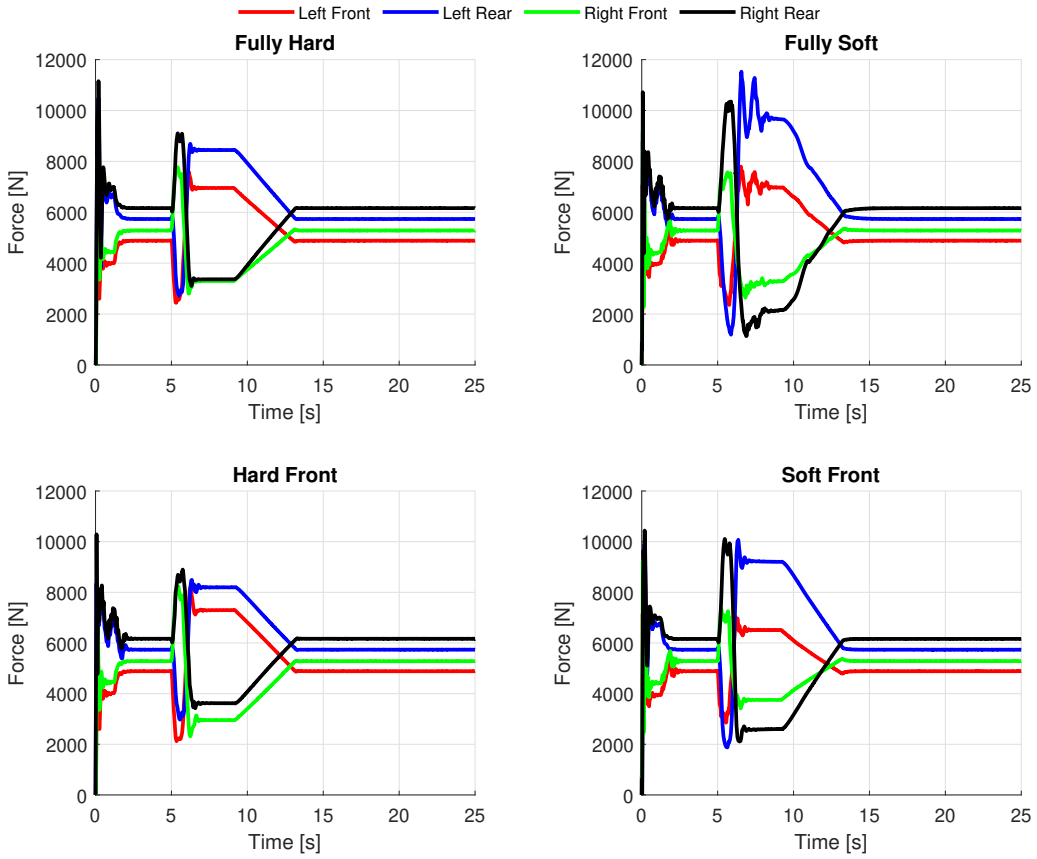

Figure 3.25. Fishhook 1B Test Vertical Tyre Forces (F_z) - 35km/h

The vertical forces observed for the soft front configuration highlight the larger vertical forces and significant load transfer at the rear of the vehicle, further confirming that this suspension setup leads to oversteer. When the vehicle enters the Fishhook manoeuvre, the soft front suspension allows for more body roll, which shifts a greater amount of weight towards the rear outside tyre. This increased load transfer amplifies the rear tyres' grip disparity compared to the front tyres, causing the rear to swing outward more readily, thereby inducing an oversteer condition. This behaviour is particularly evident in the increased yaw rate, which indicates a quicker rotation of the vehicle's rear around its vertical axis, necessitating precise driver input to maintain control. In contrast, the hard front configuration exhibits larger vertical forces and significant load transfer at the front tyres, indicating that the vehicle

experiences understeer during the manoeuvre. With a stiffer front suspension, the vehicle resists body roll more effectively, resulting in less weight being transferred to the rear. Consequently, the front tyres bear a greater proportion of the load, maintaining their grip but reducing the ability to steer sharply. This causes understeer, which causes the vehicle to follow a wider arc than intended, making it less responsive to steering inputs. The stability provided by the hard front suspension setup is beneficial for maintaining control, but it compromises the vehicle's agility in tight manoeuvres.

The fully soft configuration, which involves both front and rear suspensions being set to their softest configurations, experiences extremely large load transfer at the rear of the vehicle, exacerbating the oversteer tendency. During the Fishhook manoeuvre, the pronounced body roll results in substantial compression and rebound in the suspension struts, causing significant weight shifts. This leads to a dramatic increase in vertical forces on the rear outside tyre, reducing the overall stability of the vehicle. The resultant oversteer is evident in the yaw rate, which spikes as the rear end of the vehicle swings out more aggressively. This oversteer tendency can be corroborated by observing the vehicle's heading, which deviates more sharply from the intended path. The pronounced oversteer in the fully soft configuration is most likely due to the excessive compliance in the suspension system, allowing for large suspension travel and dynamic load changes. As the vehicle navigates through the Fishhook manoeuvre, the soft suspension permits greater body movement, leading to significant lateral load transfers. This dynamic behaviour can cause the vehicle to momentarily lose control, as the tyres struggle to maintain consistent contact with the road surface. The driver may experience a heightened sense of instability, requiring more corrective steering inputs to keep the vehicle on course.

Figure 3.26 illustrates the Land Rover's roll rate as the entry speed gradually increases. Throughout the manoeuvre, the vehicle effectively maintains control within the handling mode across all speed increments under investigation. However, it becomes apparent that the softer suspension configuration is the initial configuration that fails the test, and subsequently, as the speed increments, each configuration progressively fails, with the hard front suspension being the last to fail. This experimental evidence strongly supports the assertion that the handling mode for the suspension stands out as the most effective configuration for optimised manoeuvrability and control. The outcomes derived from the hard suspension simulation clearly demonstrate a failure in the handling mode, as evident in the observations depicted in Figure 3.27. At a speed of 50 km/h, a critical point is reached where the vehicle initiates a rollover, symbolising the termination condition due to the inside wheels lifting off the ground. Furthermore, the impact of vehicle speed on the yaw motion can be observed distinctly in

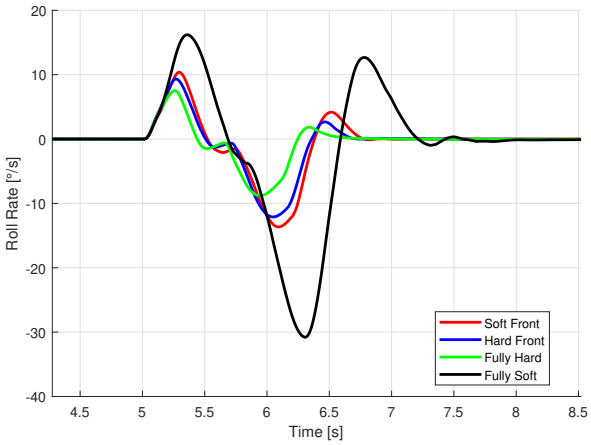

(a) Roll Rate for Suspension Configurations for 30 km/h Fishhook 1B Test

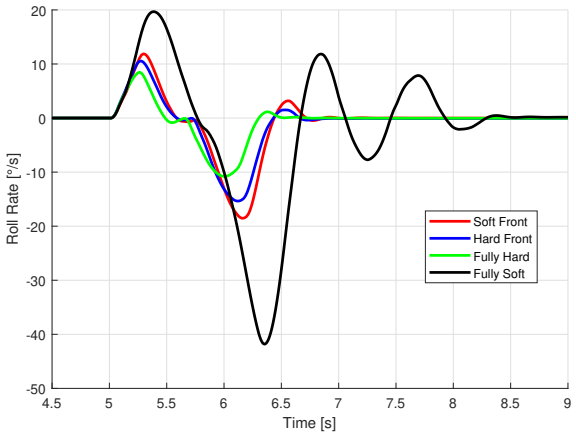

(b) Roll Rate for Suspension Configurations for 35 km/h Fishhook 1B Test

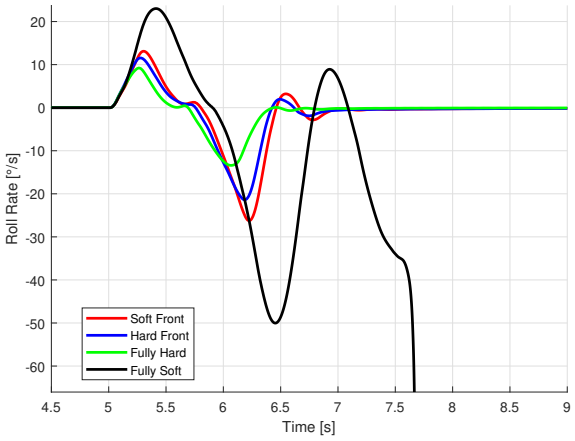

(c) Roll Rate for Suspension Configurations for 40 km/h Fishhook 1B Test

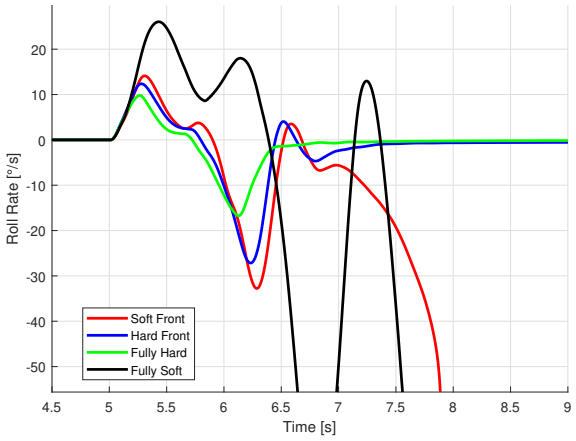

(d) Roll Rate for Suspension Configurations for 45 km/h Fishhook 1B Test

Figure 3.26. Roll Rate for Varying Suspension Configurations through NHTSA Fishhook 1B Test

Figure 3.27(d). There is a noticeable trend: as the speed escalates, the vehicle tends to navigate with a larger radius during the test manoeuvre, leading it to undergo limit oversteer. The stability of the vehicle also begins to deteriorate, notably highlighted in the examination of the roll angle and roll rate during the 45 km/h run. At this speed, the vehicle demonstrates a 'wobbling' effect throughout the manoeuvre, underscoring the significant stimulation of lateral dynamics at this critical threshold of 45 km/h.

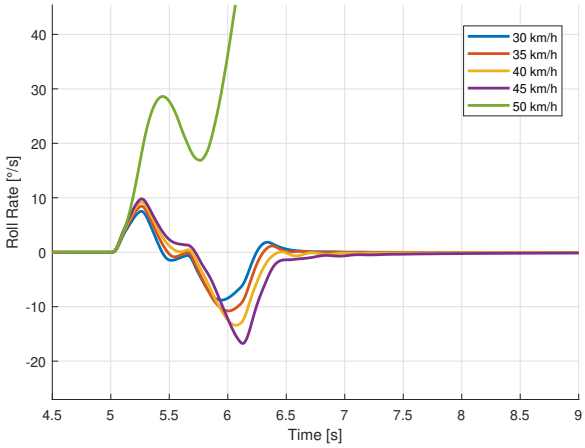

(a) Roll Rate for Hard Suspension Configuration through Fishhook 1B Test

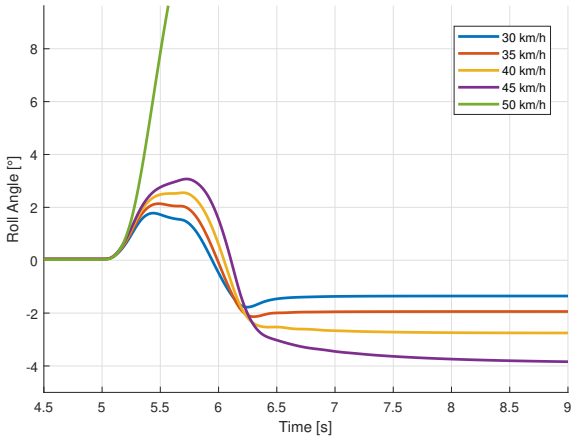

(b) Roll Angle for Hard Suspension Configuration through Fishhook 1B Test

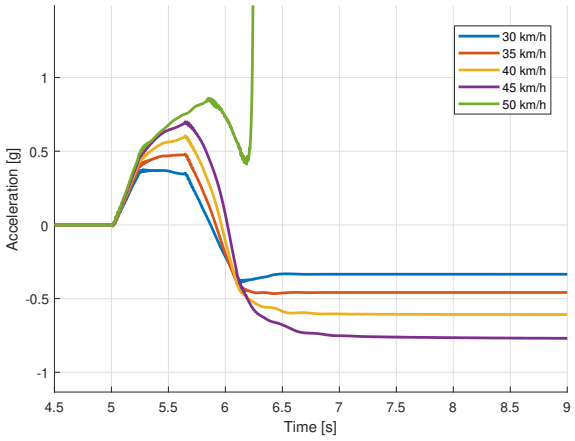

(c) Lateral Acceleration for Hard Suspension Configuration through Fishhook 1B Test

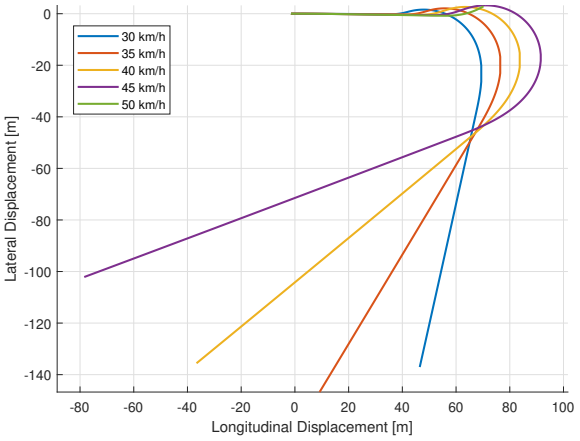

(d) Vehicle Heading for Hard Suspension Configuration through Fishhook 1B Test

Figure 3.27. Results for Hard Suspension Configuration through Fishhook 1B Test

3.5.2 Conclusion

The hard suspension configuration performs the best from the rest of the configurations by the metric that the roll rate is the lowest and this leads to the lowest roll angle, therefore the hard configuration is the safest option to mitigate rollover propensity. The hard configuration displays oversteer as the vehicle speed increases and this may be an issue in emergencies as the loss of control combined with an oversteering vehicle may lead to rollover with more probability than compared to the hard front suspension configuration. The hard front performs on par with the hard suspension and can be looked at as a more viable option than the last resort option of the fully hard suspension configuration.

4. Conclusions & Recommendations

4.1 Conclusions

The study aimed to enhance the handling performance and mitigate rollover propensity in an SUV, addressing the high incidence of accidents resulting from rollover and loss of control. It highlighted the significant impact of lateral load transfer on vehicle dynamics and rollover propensity.

The central research questions for this research were as follows:

- *Can influencing the lateral load transfer of a vehicle improve the handling characteristics and decrease the rollover propensity?*
- *Can this be achieved by implementing roll control using a semi-active suspension?*
- *How will this implementation influence the steering and handling characteristics of the vehicle?*

The implementation of suspension and ride height control in the system aimed to limit the vehicle's steer angle to the Ackermann angle of the radius of curvature and minimise the error between the front and rear tyre slip angles during steady-state cornering, thereby influencing the vehicle's understeer and oversteer characteristics. The control system focused on reducing the roll angle and lateral load transfer ratio to enhance rollover propensity and improve handling in dynamic situations.

A first-principle analysis provided a detailed depiction of how each component of the understeer gradient affected the vehicle's steering behaviour. The understeer gradient resulting from the tyre component induced an oversteer tendency when the rear weight surpassed the front weight. Interestingly, both the fully soft and fully hard configurations exhibited similar behaviours due to the linear attributes of the spring model. However, this conformity was not expected within the nonlinear suspension model, where the hard suspension configuration should resist spring compliance as the vehicle underwent increased rolling and experienced higher lateral acceleration. The soft front configuration experienced pronounced oversteer due to amplified load transfer at the rear, causing the rear tyres to lose grip more readily and making the vehicle more prone to rotating sharply. In contrast, the hard front configuration tended towards significant understeer as it encountered increased load transfer at the vehicle's front, resulting in the front tyres losing grip and causing the vehicle to turn less sharply than intended. These distinctions highlighted the varied impacts of load distribution on steering behaviour based on the suspension configuration. The fully soft configuration led to extreme load transfer at the rear during

cornering, which further exacerbated the oversteer tendency. This was because the soft suspension allowed for large body roll, significantly shifting the vehicle's weight to the rear outer tyre and reducing stability. Conversely, the fully hard configuration was expected to maintain better control over body roll, distributing the load more evenly between the tyres and thereby reducing both oversteer and understeer tendencies. However, due to the nonlinear characteristics of the suspension system, the hard suspension still exhibited some compliance, affecting handling under high lateral acceleration conditions.

These phenomena were validated and highlighted during simulations of the constant radius test where the suspension characteristics were altered, the ride height was changed, and the implementation of anti-roll control was investigated. It was found that the manipulation of the roll stiffness of an axle had a significant impact on the steering behaviour and handling dynamics of the vehicle. Both the initial order analysis and the comprehensive simulation data consistently demonstrated alignment in the trend and magnitude of these alterations. This signified the validity and credibility of modifying suspension characteristics to actively influence the distribution of load transfer within the vehicle's dynamics. The correlation between the analytical and simulated results validated the effectiveness of adjusting suspension properties to deliberately modulate the vehicle's response to lateral forces, showcasing its potential to finely tune handling characteristics and enhance overall driving performance. Implementing ride height control offered a viable avenue to actively influence and modulate the steering behaviour of a vehicle. This control mechanism presented an opportunity to induce specific handling characteristics such as understeer or oversteer by strategically adjusting the vehicle's ride height. Elevating the front or lowering the rear height configuration tended to encourage understeer tendencies, effectively influencing the vehicle's handling dynamics by promoting a propensity for a more stable, straight-line trajectory through corners. Conversely, dropping the front or elevating the rear height configuration tended to promote oversteer characteristics, which led to a more agile and responsive turning behaviour, favouring a sharper and more dynamic handling response when navigating corners or curves. Additionally, the research looked at using the varying suspension configurations during the double lane change and Fishhook 1B manoeuvres. The load transfer aspect of the altering suspension configurations was highlighted with the soft front configuration experiencing larger yaw rates, larger roll angles, and larger rear tyre vertical force differences laterally, compared to the hard front, emphasising the notion that this configuration leads to an oversteer characteristic due to the induced increase in load transfer at the rear.

Additionally, the converse is also shown with the hard front configuration experiencing lesser yaw rates, lesser roll angles, and larger front tyre vertical force differences laterally, leading to a more understeer characteristic on the vehicle.

In conclusion, the suspension and ride height control system significantly influenced the vehicle's handling characteristics by managing the load transfer dynamics and slip angles during cornering. The soft front suspension configuration led to oversteer due to increased rear load transfer, while the hard front configuration resulted in understeer due to greater front load transfer.

4.2 Recommendations

Several potential areas of future research can be explored to build on the findings of this study:

4.2.1 The impact of different types of road surfaces

To further extend the findings of this study, it is recommended to investigate the test results of SUVs under different driving scenarios, particularly those involving rough terrain. As SUVs are often used on unpaved and uneven surfaces, examining the vehicle's performance under such conditions may yield valuable insights into the impact of ride height and suspension characteristics on the rollover propensity and handling of the vehicle. Additionally, conducting further experiments and simulations with varying road profiles and terrain will allow for a more comprehensive understanding of the vehicle's behaviour and may provide additional recommendations for improving its safety and handling capabilities.

4.2.2 Improvement of the ride height control system

Moreover, the addition of the modelling of the valves and their response will lead to a more precise representation of the dynamics of the suspension system in the simulation. This will allow for more accurate control of the ride height of the vehicle, which will lead to more reliable results in terms of the reduction of rollover propensity and improvement in handling. Additionally, considering the pressure differences and the pressure accumulator in the ride height control system will enable the simulation to account for variations in road conditions, vehicle load, and other external factors that can affect the behaviour of the suspension system. This can help in designing a more robust control system that can adapt to different scenarios and improve the vehicle's safety under various conditions, and this control system will be more representative of the $4S_4$CVD.

4.2.3 Real world vehicle implementation

To progress further with this research study, the next crucial step is to validate the simulation results by conducting experimental field tests. The validation will involve conducting the defined manoeuvres in the suspension system and comparing the simulation results with the experimental results obtained using the Land Rover Defender 110 test vehicle, which has the $4S_4$CVD equipped with ride height control. This process will involve utilising the vehicle's instrumentation and data acquisition systems to gather experimental data. The validation process is necessary to ensure that the simulation results are reliable and accurate and to confirm the effectiveness of the proposed ride height control system. Moreover, the experimental results obtained will provide additional insights and information that cannot be obtained through simulations alone.

4.2.4 Control algorithm investigation and implementation:

In addition, exploring the implementation of adaptive control algorithms that can adjust the suspension characteristics in real-time based on the vehicle's dynamic behaviour and the driving conditions could potentially provide an even more effective solution for improving the safety and handling of SUVs. Adaptive control algorithms can continuously monitor and analyse parameters such as vehicle speed, road conditions, and driver inputs and adjust the suspension characteristics accordingly to optimise the vehicle's handling and stability. Such a system would be highly beneficial for SUVs as they are often used in varying driving conditions, including on and off-road, and can be subject to unpredictable road conditions such as potholes, bumps, and sudden changes in surface friction.

References

Ackermann, J. (1994), 'Robust decoupling, ideal steering dynamics and yaw stabilization of 4ws cars', *Automatica* **30**(11), 1761–1768.

Ahmadian, M. & Simon, D. E. (2004), 'Can semiactive dampers with skyhook control improve roll stability of passenger vehicles?', *SAE Transactions* **113**, 1151–1156.
URL: *http://www.jstor.org.uplib.idm.oclc.org/stable/44724940*

Balkwill, J. (2018), *Chapter 5 - Cornering*, Butterworth-Heinemann, pp. 95–179.
URL: *https://www.sciencedirect.com/science/article/pii/B9780128126936000055*

BMW M (2023), 'Game changer: The adaptive m suspension'.
URL: *https://www.bmw-m.com/en/topics/magazine-article-pool/das-adaptive-m-fahrwerk.html*

Botha, T. R. (2011), High Speed Autonomous Off-Road Vehicle Steering, Thesis, University of Pretoria.

Botha, T. R. & Els, S. (2019), 'Vehicle centre of mass, roll-centre and pitch-centre height estimation', **13**(4), 319–339.

cosin scientific software (2020), 'Ftire/core'.
URL: *https://www.cosin.eu/products/ftirecore/*

Data, S. & Frigerio, F. (2002), 'Objective evaluation of handling quality', *Proceedings of the Institution of Mechanical Engineers* **216**(4), 297–305.
URL: *https://www.proquest.com/scholarly-journals/objective-evaluation-handling-quality/docview/220682190/se-2?accountid=14717 http://UnivofPretoria.on.worldcat.org/atoztitles/link?sid=ProQ:&iss 04-01&atitle=Objective+evaluation+of+handling+quality&au=S+Data%3BFrigerio%2C+F&id=doi:*

De Wet, B. (2020), Achieving controllable continuous variable damping within a semi-active hydro-pneumatic suspension system, Dissertation, University of Pretoria.
URL: *http://hdl.handle.net/2263/81135*

Dukkipati, R. V. (2010), *Road Vehicle Dynamics*, SAE International, Warrendale, Pa.

Els, P. S. (2006), The Ride Comfort vs. Handling Compromise for Off-Road Vehicles, Thesis, University of Pretoria.
URL: *https://repository.up.ac.za/handle/2263/26302*

European Road Safety Observatory (2023), 'Electronic stability control'.
URL: *https://road-safety.transport.ec.europa.eu/european-road-safety-observatory/statistics-and-analysis-archive/esafety/electronic-stability-control_en*

Forkenbrock, G. J., Garrott, W. R., Heitz, M. & O'Harra, B. C. (2003), 'An experimental examination of j-turn and fishhook maneuvers that may induce on-road, untripped, light vehicle rollover', *SAE Transactions* **112**, 1112–1127.
URL: *http://www.jstor.org.uplib.idm.oclc.org/stable/44745487*

Forkenbrock, G., O'Harra, B. & Elsasser, D. (2004), A demonstration of the dynamic tests developed for nhtsa's ncap rollover rating system, Report, National Highway Traffic Safety Administration.

Gerrard, M. B. (1999), 'Roll centres and jacking forces in independent suspensions a first principles explanation and a designer's toolkit', *SAE Transactions* **108**, 23–34.
URL: *http://www.jstor.org.uplib.idm.oclc.org/stable/44667888*

Gillespie, T. (2021), *Fundamentals of Vehicle Dynamics*, SAE International, Warrendale, UNITED STATES.
URL: *http://ebookcentral.proquest.com/lib/pretoria-ebooks/detail.action?docID=28983770*

Gillespie, T. D. (1992), *Fundamentals of vehicle dynamics*, Society of Automotive Engineers, Warrendale, PA.
URL: *https://saemobilus.sae.org/content/R-114*

Guglielmino, E., Sireteanu, T., Stammers, C. W., Gheorghe, G. & Giuclea, M. (2008), *Semi-active Suspension Control: Improved Vehicle Ride and Road Friendliness*, 1 edn, Springer.

Hac, A. (2002), 'Rollover stability index including effects of suspension design', *JOURNAL OF PASSENGER CAR: MECHANICAL SYSTEMS JOURNAL* **111**, 1403–1413.
URL: *https://www.jstor.org/stable/44719316*

Hamersma, H. A. (2013), Longitudinal vehicle dynamics control for improved vehicle safety, Thesis.

Haney, P. (2012), *The racing and high-performance tire using the tires to tune for grip and balance*, Infotire, Dallas, Tex.

Hexagon (2023), 'Adams'.
URL: *https://hexagon.com/products/product-groups/computer-aided-engineering-software/adams*

Hwang, H.-Y., Tian-Syung, L. & Chen, J.-S. (2020), 'Developing a strategy to improve handling behaviors of a medium-size electric bus using active anti-roll bar', *Symmetry* **12**(8), 1334.
URL: *https://www.proquest.com/scholarly-journals/developing-strategy-improve-handling-behaviors/docview/2434217252/se-2?accountid=14717*

Insurance Institute for Highway Safety (2020), 'Fatality facts 2020: Passenger vehicle occupants'.
URL: *https://www.iihs.org/topics/fatality-statistics/detail/passenger-vehicle-occupants#rollover*

International Organization for Standardization (1999), *Passenger cars - test track for a severe lane-change manoeuvre - : Part 1: Double lane-change*, International standard ; ISO 3888-1, 1st ed. 1999-10-01. edn, International Organization for Standardization, Geneva, Switzerland.

International Organization for Standardization (2011), *Road vehicles - Lateral transient response test methods - open-loop test methods*, International standard ; ISO 7401:2011, 3rd ed. 2011-04-15. edn, International Organization for Standardization, Geneva, Switzerland.

International Organization for Standardization (2012), *Passenger cars - Steady-state circular driving behaviour - Open-loop test methods*, International standard ; ISO 4138:2012, 4th ed. 2012-06-01. edn, International Organization for Standardization, Geneva, Switzerland.

Isermann, R. (2022), *Automotive control: modeling and control of vehicles*, Springer.

Kapania, N. R. & Gerdes, J. C. (2015), 'Design of a feedback-feedforward steering controller for accurate path tracking and stability at the limits of handling', *Vehicle System Dynamics* **53**(12), 1687–1704.
URL: *https://doi.org/10.1080/00423114.2015.1055279*

Karimi Eskandary, P., Khajepour, A., Wong, A. & Ansari, M. (2016), 'Analysis and optimization of air suspension system with independent height and stiffness tuning', *International Journal of Automotive Technology* **17**(5), 807–816.
URL: *https://doi.org/10.1007/s12239-016-0079-9*

Kim, C. & Huh, K. (2019), 'Active roll control system design with considering actuator constraints for passenger car', *Journal of Dynamic Systems, Measurement, and Control* **141**(12).
URL: *https://doi.org/10.1115/1.4044461*

Lapapong, S., Brown, A. A., Swanson, K. S. & Brennan, S. N. (2012), 'Zero-moment point determination of worst-case manoeuvres leading to vehicle wheel lift', *Vehicle System Dynamics* **50**, 191–214.

Larish, C., Piyabongkarn, D., Tsourapas, V. & Rajamani, R. (2013), 'A new predictive lateral load transfer ratio for rollover prevention systems', *IEEE Transactions on Vehicular Technology* **62**(7), 2928 – 2936.
URL: *https://ieeexplore.ieee.org/document/6480893*

Lee, D., Jin, S. W., Rhee, E.-j. & Lee, C. (2021), 'Practical damper velocity estimation for semi-active suspension control', *International Journal of Automotive Technology* **22**(2), 499–506.
URL: *https://doi.org/10.1007/s12239-021-0046-y*

Lee, G.-w., Hyun, M., Kang, D.-o. & Heo, S.-j. (2022), 'High-efficiency active suspension based on continuous damping control', *International Journal of Automotive Technology* **23**(1), 31–40.
URL: *https://doi.org/10.1007/s12239-022-0003-4*

Liu, H., Gao, H. & Li, P. (2014), *Handbook of Vehicle Suspension Control Systems*, Institution of Engineering and Technology (The IET).

URL: *https://app.knovel.com/hotlink/pdf/id:kt00C3JTC2/handbook-vehicle-suspension/evaluation-criterion*

Ma, X., Wong, P. K., Zhao, J., Zhong, J.-H., Ying, H. & Xu, X. (2018), 'Design and testing of a nonlinear model predictive controller for ride height control of automotive semi-active air suspension systems', *IEEE Access* **6**.

Milliken, D. L. & Milliken, W. F. (2003), *Race car vehicle dynamics : problems, answers, and experiments*, SAE International, Warrendale, PA.

Multimatic Inc. (2023), 'Dssv damping technology'.
URL: *https://www.multimatic.com/manufacturing/suspension/damping-technology/*

Pacejka, H. B. & Bakker, E. (1992), 'The magic formula tyre model', *Vehicle System Dynamics* **21**(sup001), 1–18.
URL: *https://doi.org/10.1080/00423119208969994*

Reimpell, J. & Stoll, H. (1996), *The automotive chassis : engineering principles : types of drive and suspension, tyres and wheels, axle kinematics, steering, springing, chassis and vehicle overall*, Arnold, London.

S. Minjun, Y. Changhee, P. S.-S. & Kanghyun, N. (2018), 'Development of wheel pressure control algorithm for electronic stability control (esc) system of commercial trucks', *SAE Transactions* **18**(7), 2317.

SAE International (2018), 'Steady-state directional control test procedures for passenger cars and light trucks', **J266_201811**.
URL: *https://www.sae.org/standards/content/j266_201811/*

Sakai, H. & Satoh, Y. (1994), 'The impact of roll center height on vehicle dynamic behavior', *JSAE Review* **15**(4), 329–333.

Sanghyun, H., Chankyu, L., Borrelli, F. & Hedrick, J. K. (2015), 'A novel approach for vehicle inertial parameter identification using a dual kalman filter', *IEEE Transactions on Intelligent Transportation Systems* **16**(1).

Schmeitz, A., Besselink, I., Hoogh, J. & Nijmeijer, H. (2005), 'Extending the magic formula and swift tyre models for inflation pressure changes'.

Statista (2023), 'Sport utility vehicles worldwide - statistics & facts'.
URL: *https://www.statista.com/topics/6185/suv-market-worldwide/topicOverview*

Tandy, D. F., Colborn, J., Bae, J. C., Coleman, C., Pascarella, R., Congress, S. A. E. W. & Exhibition Detroit, M. U. S. (2015), 'The true definition and measurement of oversteer and understeer', *SAE International Journal of Commercial Vehicles* **8**(1), 160–181.

Thoresson, M. J. (2007), Efficient gradient-based optimisation of suspension characteristics for an off-road vehicle, Thesis.
URL: *http://hdl.handle.net/2263/26984*

Tian, S., Lang, W., Schwarz, C., Zhou, W., Jiao, Y. & Chen, Y. (2018), 'An earlier predictive rollover index designed for bus rollover detection and prevention', *Journal of Advanced Transportation* **2018**, 10.
URL: *https://www.proquest.com/scholarly-journals/earlier-predictive-rollover-index-designed-bus/docview/2407646464/se-2?accountid=14717*

Uys, P. E., Els, P. S., Theron, N. J. & Thoresson, M. J. (2007), 'The ride comfort vs. handling compromise for off-road vehicles', *Journal of Terramechanics* **44**(4), 303–317.
URL: *https://www.sciencedirect.com/science/article/pii/S0022489807000213*

Uys, P. E., Els, P. S., Thoresson, M. J., Voigt, K. G. & Combrinck, W. C. (2006), 'Experimental determination of moments of inertia for an off-road vehicle in a regular engineering laboratory', *International Journal of Mechanical Engineering Education* **34**(4), 291–314.

Vahidi, A., Stefanopoulou, A. & Peng, H. (2005), 'Recursive least squares with forgetting for

online estimation of vehicle mass and road grade: theory and experiments', *Vehicle System Dynamics* **43**(1), 31–55.

Van Der Sande, T. P. J., Merks, M. H. M., Lindeman, E. & Nijmeijer, H. (2022), 'Rule-based control of a semi-active suspension system for road holding using limited sensor information: design and experiments', *Vehicle System Dynamics* **60**(12), 4226–4244.
URL: *https://doi.org/10.1080/00423114.2021.2007270*

VBOX Automotive (2023), 'Vbox 3i 100 hz gnss data logger'.
URL: *https://www.vboxautomotive.co.uk/index.php/en/products/data-loggers/vb3i*

Vosloo, A. G. (2019), Hydropneumatic semi-active suspension system with continuously variable damping, Dissertation, University of Pretoria.
URL: *http://hdl.handle.net/2263/73167*

Vu, V. T., Sename, O., Dugard, L. & Gaspar, P. (2016), 'Active anti-roll bar control using electronic servo valve hydraulic damper on single unit heavy vehicle', *IFAC-PapersOnLine* **49**(11), 418–425.
URL: *https://www.sciencedirect.com/science/article/pii/S2405896316314021*

Wang, C., Wang, Z., Zhang, L., Cao, D. & Dorrell, D. G. (2021), 'A vehicle rollover evaluation system based on enabling state and parameter estimation', *IEEE Transactions on Industrial Informatics* **17**(6).

Wang, J. & Shen, S. (2008), 'Integrated vehicle ride and roll control via active suspensions', *Vehicle System Dynamics* **46**(sup1), 495–508.
URL: *https://doi.org/10.1080/00423110801993128*

Widner, A. & Bári, G. (2018), 'Investigating the effects of roll center height in simulation, for safety-margin research', *IOP Conference Series. Materials Science and Engineering* **393**(1).

Wittmer, K., Sawodny, O. & Henning, K.-U. (2023), 'Model-based estimation of vehicle center of gravity height and load', *J. Dyn. Sys., Meas., Control* **145**(5).

Wong, J. Y. (2013), *Theory of Ground Vehicles*, John Wiley & Sons, Inc.
URL: *https://www.wiley.com/en-br/Theory+of+Ground+Vehicles,+5th+Edition-p-9781119719700*

Wright, K. R., Botha, T. R. & Els, P. S. (2019), 'Effects of age and wear on the stiffness and friction properties of an suv tyre', *Journal of Terramechanics* **84**, 21–30.
URL: *https://www.sciencedirect.com/science/article/pii/S0022489817301623*

Wu, X., Farhad, M. & Wong, J. (2011), 'Investigating and improving vehicle transient handling performance', *SAE International Journal of Materials and Manufacturing* **4**(1), 1080–1098.
URL: *http://www.jstor.org.uplib.idm.oclc.org/stable/26273842*

Xu, X., Chen, L., Sun, L. & Sun, X. (2013), 'Dynamic ride height adjusting controller of ecas vehicle with random road disturbances', *Mathematical Problems in Engineering* **2013**.

Yoon, J., Cho, W., Kang, J., Koo, B. & Yi, K. (2010), 'Design and evaluation of a unified chassis control system for rollover prevention and vehicle stability improvement on a virtual test track', *Control Engineering Practice* **18**(6), 585–597.
URL: *https://www.sciencedirect.com/science/article/pii/S0967066110000729*

Yu, H., Guvenc, L. & Ozguner, U. (2008), 'Heavy duty vehicle rollover detection and active roll control', *Vehicle System Dynamics* **46**(6), 451–470.
URL: *https://doi.org/10.1080/00423110701477529*

Zhang, X., Yang, Y., Guo, K., Lv, J. & Peng, T. (2017), 'Contour line of load transfer ratio for vehicle rollover prediction', *Vehicle System Dynamics* **55**(11), 1748–1763.